

Targeting HER2

A report on the in vitro and in vivo pre-clinical data supporting trastuzumab as a radioimmunoconjugate for clinical trials

Diane E. Milenic,^{1,*} Karen J. Wong,² Kwamena E. Baidoo,¹ Tapan K. Nayak,¹ Celeste A.S. Regino,² Kayhan Garmestani¹ and Martin W. Brechbiel¹

¹Radioimmune and Inorganic Chemistry Section; Radiation Oncology Branch; and ²Molecular Imaging Program; Center for Cancer Research; National Cancer Institute; National Institutes of Health; Bethesda, MD USA

Key words: monoclonal antibody, HER2, trastuzumab, radioimmunodiagnosis, radioimmunotherapy

The potential of the HER2-targeting antibody trastuzumab as a radioimmunoconjugate useful for both imaging and therapy was investigated. Conjugation of trastuzumab with the acyclic bifunctional chelator CHX-A^{99m}-DTPA yielded a chelate:protein ratio of 3.4 ± 0.3 ; the immunoreactivity of the antibody unaffected. Radiolabeling was efficient, routinely yielding a product with high specific activity. Tumor targeting was evaluated in mice bearing subcutaneous (s.c.) xenografts of colorectal, pancreatic, ovarian and prostate carcinomas. High uptake of the radioimmunoconjugate, injected intravenously (i.v.), was observed in each of the models and the highest tumor %ID/g (51.18 ± 13.58) was obtained with the ovarian (SKOV-3) tumor xenograft. Specificity was demonstrated by the absence of uptake of ¹¹¹In-trastuzumab by melanoma (A375) s.c. xenografts and ¹¹¹In-HuIgG by s.c. LS-174T xenografts. Minimal uptake of i.v. injected ¹¹¹In-trastuzumab in normal organs was confirmed in non-tumor-bearing mice. The in vivo behavior of ¹¹¹In-trastuzumab in mice bearing intraperitoneal (i.p.) LS-174T tumors resulted in a tumor %ID/g of 130.85 ± 273.34 at 24 h. Visualization of tumor, s.c. and i.p. xenografts was achieved by γ -scintigraphy and PET imaging. Blood pool was evident as expected but cleared over time. The blood pharmacokinetics of i.v. and i.p. injected ¹¹¹In-trastuzumab was determined in mice with and without tumors. The data from these in vitro and in vivo studies supported advancement of radiolabeled trastuzumab into two clinical studies, a Phase 0 imaging study in the Molecular Imaging Program of the National Cancer Institute and a Phase 1 radioimmunotherapy study at the University of Alabama.

Introduction

In 1998, anti-HER2 trastuzumab (Herceptin[®], Roche) became the first humanized monoclonal antibody (mAb) to gain US Food and Drug Administration (FDA) approval. Trastuzumab, as a single agent, is indicated for the treatment of patients with metastatic breast cancer whose tumors overexpress the HER2 protein and who have received one or more chemotherapy regimens. Trastuzumab is also approved for use in combination with paclitaxel for the treatment of patients with HER2 expressing metastatic breast cancer who have not received chemotherapy for their metastatic disease.

HER2, a transmembrane receptor tyrosine kinase, is overexpressed in 25–30% of breast cancers. Patients are selected for trastuzumab therapy using immunohistochemical (IHC) staining or fluorescence in situ hybridization (FISH), which probes for either the expression of HER2 or amplification of the HER2 gene.¹ Using the IHC technique, the patient's tumor HER2

expression must score a 2+ or 3+ to be eligible for therapy.² Of those patients receiving trastuzumab as a single agent, only 12–35% of the patients respond; however, when combined with paclitaxel, response rates have been 40–60%.³ This response rate is further complicated by the fact that the majority of the patients who initially respond to trastuzumab therapy will experience progression of their disease within 1 year of beginning therapy with the mAb.⁴ The mechanism(s) of this resistance is yet to be understood.⁵

Radiolabeled mAbs, whether used in imaging or in therapeutic applications, do not share the same constraints as “naked,” i.e., unmodified, mAbs. Foremost, not all tumor cells need to express the target antigen, nor is high expression of that antigen required. In radioimmunotherapy (RIT), particle decay is omnidirectional and adjacent cells regardless of HER2 expression may receive a cytotoxic dose. Furthermore, irradiation of cells results in stress signaling that also affects neighboring cells.^{6,7} This dual bystander effect not only overcomes the heterogeneity of antigen

*Correspondence to: Diane E. Milenic; Email: dm71q@nih.gov

Submitted: 05/21/10; Accepted: 07/19/10

Previously published online: www.landesbioscience.com/journals/mabs/article/13054

DOI: 10.4161/mabs.2.5.13054

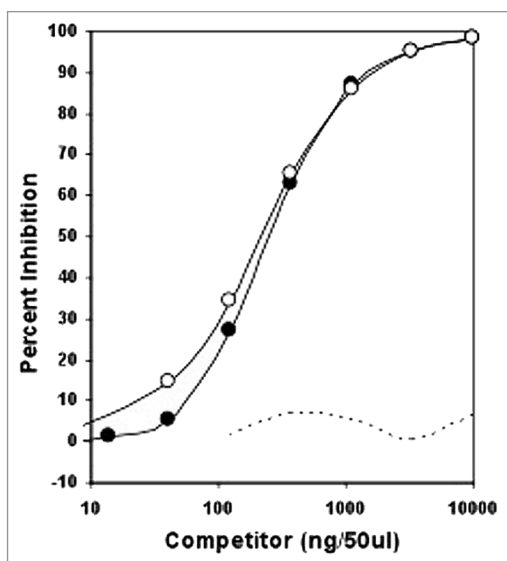


Figure 1. Analysis of trastuzumab immunoreactivity. The immunoreactivity of trastuzumab-CHX-A''DTPA (open circle) for HER2-expressing (fixed) SKOV-3 cells was evaluated in a competition radioimmunoassay. The trastuzumab-CHX-A''DTPA was compared to unmodified trastuzumab (closed circle); the anti-CD33 mAb, HuM195, (dotted line) served as a negative control.

expression within a tumor mass but also, in some part, overcomes accessibility barriers.

The potential of HER2 as a target extends beyond breast cancer, as HER2 is not only overexpressed in breast cancer but also in ovarian (25–30%), pancreatic (35–45%), colorectal (up to 90%) and an array of other epithelial cancers.^{8,9} In theory, patients that score 1+ or even ± could potentially benefit from therapy with trastuzumab labeled with either an α - or β -particle emitting radionuclide. Studies from this laboratory and others have demonstrated such tumor targeting, as well as therapeutic efficacy.¹⁰⁻¹⁹ A wider population of patients might benefit from therapy with trastuzumab and trastuzumab-targeted therapies.

Radiolabeling trastuzumab with γ - or β^+ -emitting radionuclides provides a means to visualize and quantitate the HER2 target with a non-invasive methodology.^{12,17,18,20-29} Radiolabeled trastuzumab may be exploited as a tool in nuclear medicine to (1) monitor treatment responses of patients, (2) determine the emergence of resistance and therefore treatment failure, (3) make dosimetric calculations and predictions for radioimmunotherapeutic regimens, (4) detect distal or metastatic disease, (5) restage a patient's disease, (6) select patients for targeted therapy and finally, (7) identify those patients at risk, i.e., cardiac toxicity.

The objective of the work presented herein was 2-fold. The first aspect was to provide convincing data advocating the potential of radiolabeled trastuzumab for imaging and therapy that would benefit a greater population of cancer patients. The second was to present the data that serves as the foundation for two clinical studies. The first is an ongoing Phase 0 imaging study (NCI-07-C-0101) conducted in collaboration with the National Cancer Institute's (NCI) Molecular Imaging Program. The trial

is designed to establish the safety of ¹¹¹In-trastuzumab, determine the optimal timing of imaging as a function of HER2 status, correlate uptake with traditional immunohistochemistry (IHC) assessment of HER2 status, determine biodistribution of the agent in normal organs and determine the pharmacokinetics of serum clearance. The second clinical study will be conducted at the University of Alabama by Dr. Ruby Meredith in collaboration with AREVA Med LLC (Paris, France). In this Phase I study, escalating doses of ²¹²Pb-trastuzumab will be administered to ovarian cancer patients by intraperitoneal (i.p.) injection to establish safety and a maximum tolerated dose.

Results

Trastuzumab conjugation with CHX-A''DTPA, radiolabeling and in vitro characterization. Conjugation of trastuzumab with the acyclic ligand, CHX-A''DTPA, was initially performed using a molar excess (10-fold) of the ligand to the mAb. This reaction resulted in a final product with a chelate:protein ratio of 3.1. Subsequent conjugations (~6) have continued to be performed at a 10:1 molar excess of CHX-A''DTPA to trastuzumab, yielding an immunoconjugate with an average chelate:protein ratio of 3.4 ± 0.3 . Analysis of the trastuzumab-CHX-A''DTPA conjugate by a competition radioimmunoassay indicated that modification of trastuzumab with this number of chelates did not affect the immunoreactivity of the mAb (Fig. 1).

Routine radiolabeling of the trastuzumab-CHX-A''DTPA preparations have resulted in a % incorporation of 79.6 ± 6.6 with a specific activity of 17.8 ± 4.7 mCi/mg for ¹¹¹In and a 44.8% incorporation of ⁸⁶Y with a specific activity of 18.7 ± 13.2 mCi/mg. Analysis of the radioimmunoconjugate (RIC) by size-exclusion high performance liquid chromatography (HPLC) revealed that the radioactivity had a retention time consistent with intact IgG with <2% (each) associated with higher and lower molecular weight species (data not shown).

Immunoreactivity of the RIC was evaluated in a radioimmunoassay using fixed HER2-positive (SKOV-3). Following an overnight incubation at ambient temperature, $55.3 \pm 14.5\%$ of the radioactivity was bound to the HER2 positive cells. Addition of 10 μ g of unlabeled trastuzumab blocked the binding; only $12.5 \pm 8.8\%$ of the radioactivity remained bound to the cells, thus demonstrating specificity.

In anticipation of clinical trials, a study was conducted evaluating the affect of specific activity on the integrity and immunoreactivity of trastuzumab. 25 μ g of trastuzumab was radiolabeled with amounts of ¹¹¹In ranging from 110–5,120 μ Ci; the resulting specific activities ranged from 4.95–177.5 mCi/mg. No loss of immunoreactivity (54–61.7% binding) was observed when the antibodies were assayed with HER2 expressing cells; at the same time, the non-specific binding remained low (<10%). When analyzed by size-exclusion HPLC, the radioactivity was found to remain associated with the IgG peak (retention time ~12.7 min) and neither higher nor lower molecular species were evident (data not shown).

In vivo behavior of ¹¹¹In-trastuzumab. Athymic mice bearing subcutaneous (s.c.) LS-174T xenografts (n = 5) were injected

Table 1. Tumor targeting and normal organ distribution of ¹¹¹In-trastuzumab following i.v. administration in athymic mice, non-tumor-bearing and bearing s.c. LS-174T xenografts

| Non-tumor-bearing mice | | | | | |
|------------------------|---------------------------|--------------|--------------|--------------|--------------|
| Tissue | Time points (h) | | | | |
| | 24 | 48 | 72 | 96 | 168 |
| Blood | 17.95 (1.87) ^a | 19.11 (2.55) | 16.14 (3.35) | 18.18 (2.03) | 12.07 (3.94) |
| Brain | 0.46 (0.06) | 0.62 (0.14) | 0.43 (0.08) | 0.53 (0.04) | 0.30 (0.11) |
| Liver | 6.66 (1.20) | 6.80 (0.51) | 5.99 (1.90) | 5.44 (3.05) | 4.23 (1.10) |
| Spleen | 8.49 (3.04) | 8.52 (2.02) | 5.97 (1.91) | 10.02 (2.15) | 5.64 (1.99) |
| Kidneys | 6.03 (0.32) | 6.61 (0.60) | 5.58 (0.96) | 8.97 (6.42) | 4.42 (1.33) |
| Lungs | 8.06 (1.26) | 7.66 (1.52) | 7.15 (2.14) | 7.70 (2.70) | 5.23 (2.64) |
| Heart | 5.48 (0.63) | 6.03 (1.08) | 5.26 (1.20) | 8.34 (5.99) | 3.90 (1.35) |
| Stomach | 3.03 (0.80) | 2.60 (0.24) | 1.98 (0.39) | 3.47 (2.31) | 1.79 (0.48) |
| Small Intestine | 3.76 (1.66) | 2.05 (0.75) | 2.09 (0.34) | 2.28 (0.88) | 1.45 (0.57) |
| Large Intestine | 3.03 (0.91) | 4.72 (4.61) | 1.86 (0.12) | 2.31 (0.44) | 1.40 (0.49) |
| Ovaries | 4.80 (0.92) | 5.49 (1.23) | 4.81 (1.39) | 8.67 (7.71) | 3.79 (2.15) |
| Uterus | 8.36 (4.14) | 8.44 (2.39) | 6.01 (1.30) | 6.80 (2.73) | 4.78 (1.76) |
| Urinary Bladder | 3.91 (1.21) | 5.14 (2.73) | 3.77 (1.32) | 6.91 (5.82) | 2.83 (1.00) |
| Muscle | 1.97 (0.32) | 1.82 (0.19) | 1.59 (0.18) | 2.21 (1.50) | 0.94 (0.24) |
| Skin | 6.62 (0.57) | 6.08 (0.57) | 5.42 (1.03) | 4.03 (2.10) | 3.58 (0.74) |
| Axillary Lymph Nodes | 6.15 (2.34) | 6.82 (5.04) | 3.83 (0.78) | 8.14 (4.79) | 3.57 (1.21) |
| Femur | 3.56 (0.78) | 3.15 (0.48) | 2.16 (0.44) | 4.33 (4.64) | 1.63 (0.42) |
| Salivary | 6.67 (1.07) | 7.50 (1.13) | 6.55 (1.08) | 6.16 (3.62) | 4.97 (2.05) |
| Tumor-bearing mice | | | | | |
| Tissue | Time points (h) | | | | |
| | 24 | 48 | 72 | 120 | 168 |
| Blood | 10.54 (1.32) | 8.58 (1.17) | 7.49 (3.00) | 3.32 (0.81) | 1.45 (1.45) |
| Tumor | 29.00 (14.85) | 35.02 (6.51) | 32.99 (7.26) | 22.45 (3.36) | 26.94 (4.27) |
| Liver | 5.83 (1.10) | 6.16 (2.64) | 6.94 (1.74) | 6.51 (1.58) | 6.93 (3.09) |
| Spleen | 3.14 (0.36) | 4.13 (1.04) | 4.42 (1.51) | 2.59 (0.38) | 2.79 (1.16) |
| Kidneys | 2.27 (0.22) | 2.25 (0.77) | 2.15 (0.45) | 1.34 (0.14) | 1.53 (0.37) |
| Lungs | 3.60 (0.27) | 3.93 (0.99) | 3.20 (0.63) | 1.73 (0.27) | 1.69 (0.95) |
| Heart | 2.90 (0.48) | 2.59 (0.57) | 2.26 (0.83) | 1.14 (0.83) | 1.33 (0.33) |
| Stomach | 1.09 (0.11) | 1.15 (0.25) | 1.49 (0.28) | 0.59 (0.28) | 0.63 (0.28) |
| Small Intestine | 1.10 (0.29) | 1.19 (0.43) | 1.30 (0.45) | 0.60 (0.45) | 0.66 (0.29) |
| Large Intestine | 0.99 (0.17) | 1.17 (0.61) | 1.42 (0.60) | 0.57 (0.60) | 0.71 (0.35) |
| Ovaries | 2.93 (0.78) | 3.55 (1.43) | 3.74 (0.91) | 2.36 (0.91) | 1.85 (1.10) |
| Uterus | 3.08 (0.41) | 4.30 (1.42) | 5.84 (4.12) | 7.97 (4.12) | 3.51 (2.08) |
| Urinary Bladder | 2.49 (0.49) | 3.74 (1.24) | 3.60 (1.15) | 1.66 (1.15) | 1.59 (0.72) |
| Femur | 1.39 (0.32) | 1.86 (1.06) | 1.63 (0.34) | 1.77 (1.68) | 0.99 (0.40) |
| Thyroid | 2.37 (0.28) | 2.37 (0.98) | 3.53 (1.00) | 2.03 (1.00) | 1.66 (0.85) |

^aAthymic mice bearing s.c. LS-174T (0.4–0.6 cm diameter) xenografts and non-tumor-bearing mice were injected (i.v.) with ¹¹¹In-trastuzumab (~7.5 μCi/2.3 μg trastuzumab). The mice were sacrificed by exsanguination, the blood and tissues were harvested, wet-weighted and the radioactivity measured. The values represent the average percent injected dose per gram of tissue (%ID/g). The standard deviations were also calculated and are given in parentheses.

intravenously (i.v.) with ¹¹¹In-trastuzumab to define the tumor targeting and normal organ distribution of the radioimmunoconjugate (RIC). Excellent tumor targeting of ¹¹¹In-trastuzumab was observed, with a peak tumor %ID/g of 35.02 ± 6.51 at 48 h (Table 1). Throughout the study period, the tumor %ID/g

remained high with a final value of 26.94 ± 4.27 at 168 h. Of the normal organs, the highest %ID/g was observed in the blood (10.54 ± 1.32) at 24 h, which then decreased to 1.45 ± 1.45 by 168 h. The next highest %ID/g was observed in the uterus, with a value of 7.97 ± 0.13 noted at 120 h. Among the remainder of the normal

Table 2. Biphasic analysis of blood pharmacokinetics of ^{111}In -trastuzumab following i.v. or i.p. administration

| | Intravenous injection | | | Intraperitoneal injection | | |
|-------------------|-----------------------|---------|-------|---------------------------|---------|-------|
| | α^a | β | r^2 | α | β | r^2 |
| Non-tumor-Bearing | 1.2 | 160.7 | 0.954 | 10.0 | 66.9 | 0.998 |
| Tumor Bearing | 0.6 | 57.1 | 0.983 | 2.5 | 33.2 | 0.998 |

^aNon-tumor-bearing mice or mice bearing s.c. LS-174T xenografts were injected by intravenous or intraperitoneal injection with $\sim 7.5 \mu\text{Ci}$ of ^{111}In -trastuzumab ($\sim 2.3 \mu\text{g}$). Blood samples ($10 \mu\text{L}$) were drawn over 1–2 week period and measured in a γ -counter. The $\% \text{ID}/\text{mL}$ was plotted and the α - and β - values calculated using SigmaPlot 2001.

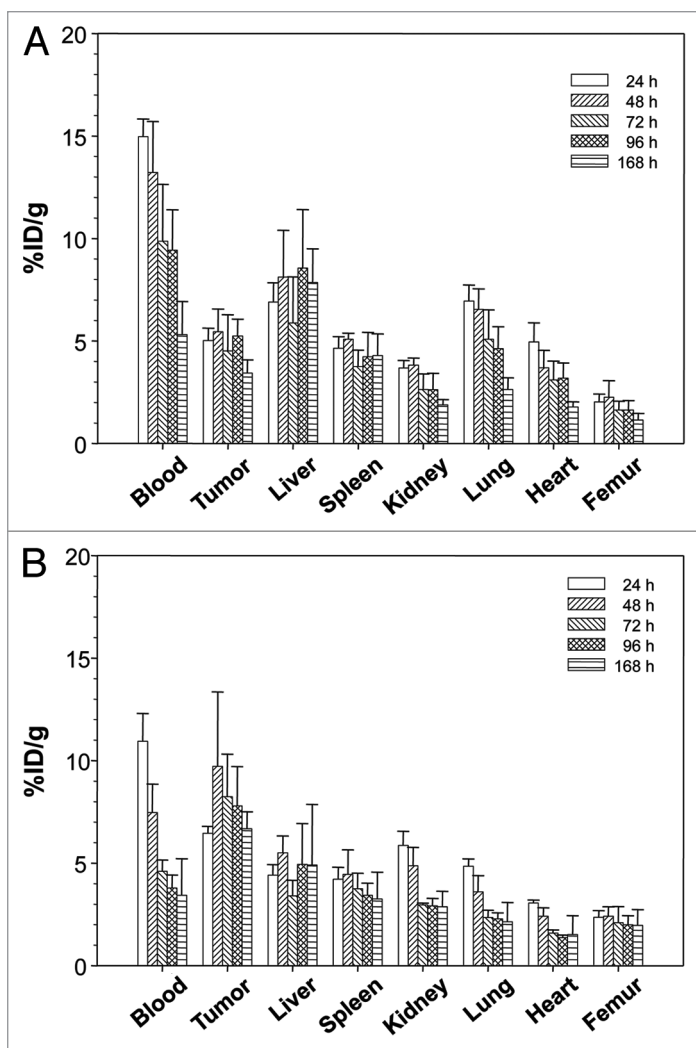


Figure 2. Specificity of ^{111}In -trastuzumab was demonstrated by performing biodistributions with a non-specific antibody and with HER2 negative xenograft. A non-specific antibody, HulGg (Top Part), was radiolabeled with ^{111}In and administered to athymic mice bearing s.c. LS-174T tumors by i.v. administration ($\sim 7.5 \mu\text{Ci}/2 \mu\text{g}$ HulGg) when the tumors measured 0.4–0.6 cm in diameter. In a second experiment, mice bearing HER2 negative s.c. melanoma (A375) xenografts were given i.v. injections of ^{111}In -trastuzumab ($\sim 7.5 \mu\text{Ci}/2.3 \mu\text{g}$ trastuzumab; Bottom Part). Mice ($n = 5$) were euthanized at the indicated times, blood, tumor and organs were harvested, wet-weighted and the radioactivity measured. The $\% \text{ID}/\text{g}$ with the standard deviations plotted.

organs, the liver presented with the next highest $\% \text{ID}/\text{g}$ (6.94 ± 1.74) at 72 h; values were less than 5 for other organs.

The normal organ distribution of ^{111}In -trastuzumab was also evaluated in non-tumor-bearing athymic mice. Mice were injected with $\sim 7.5 \mu\text{Ci}$ of the RIC and euthanized at 24, 48, 72, 96 and 168 h for a comprehensive organ harvest. The highest $\% \text{ID}/\text{g}$ (19.11 ± 2.55) was obtained in the blood at 48 h which decreased to 12.07 ± 3.94 by the end of the 168 h study (Table 1). In fact, there seemed to be no difference in the amount of the RIC in the blood until 168 h. The next highest $\% \text{ID}/\text{g}$ was observed in the spleen (10.02 ± 2.15) 96 h post-injection. Overall, with the exception of the liver, the normal organs presented with a higher $\% \text{ID}/\text{g}$ than their counterparts in the tumor-bearing mice.

The blood pharmacokinetics of i.v. administered ^{111}In -trastuzumab were evaluated in mice bearing LS-174T (s.c.) xenografts and in non-tumor-bearing mice. As illustrated by the data presented in Table 2, it is apparent that there was a longer residence time of the RIC in the blood compartment when tumor was not present. The $T_{1/2\alpha}$ and $T_{1/2\beta}$ phases were 2-fold and 2.8-fold higher, respectively, in the non-tumor-bearing mice.

Specificity of ^{111}In -trastuzumab tumor targeting. Specificity of trastuzumab tumor targeting was validated using two experimental designs. First, mice bearing s.c. LS-174T xenografts were injected i.v. with ^{111}In -labeled HulGg and then, over the course of a week, euthanized for analysis of their tumors and normal tissues. The results of this study are illustrated in Figure 2A. Overall, the level of ^{111}In -HulGg in the blood is comparable to that of ^{111}In -trastuzumab. The $\% \text{ID}/\text{g}$ at 24 h was 14.96 ± 0.87 , which steadily decreased to 5.30 ± 1.62 at the end of the 168 h study. The liver resulted in the highest $\% \text{ID}/\text{g}$, with a value of 8.55 ± 2.86 at 96 h. The maximum $\% \text{ID}/\text{g}$ for the tumor xenograft was 5.45 ± 2.86 , which was observed at 48 h. The lungs also had a higher value than the tumor at the 24 h time point.

The second experiment involved injecting (i.v.) mice bearing s.c. melanoma (A375) xenografts with ^{111}In -trastuzumab (Fig. 2B). As with the previous experiment, the highest level of the RIC in the blood was noted at 24 h (10.94 ± 1.35), which cleared to 3.43 ± 1.79 by 168 h. In the tumor, the peak $\% \text{ID}/\text{g}$ (9.73 ± 3.62) occurred at 48 h and ended with 6.67 ± 0.84 at 168 h. The uptake in the normal organs was low, comparable to what had been observed in the other tumor xenograft models.

Potential of ^{111}In -trastuzumab for the targeting of other cancers. The tumor targeting potential of ^{111}In -trastuzumab was assessed in five additional tumor s.c. xenograft models representing ovarian (SKOV-3), pancreatic (PC-Sw), colorectal (HT-29) and prostate cancer (DU-145 and PC-3). The results of these experiments are outlined in Figure 3 and Table 3. In each of the models investigated, tumor targeting was found to be comparable to or greater than what was observed with the LS-174T model. The highest tumor $\% \text{ID}/\text{g}$ obtained was with the SKOV-3 xenograft at the 96 hr time point (51.18 ± 13.58) while the PC-3 xenograft resulted in the lowest $\% \text{ID}/\text{g}$ with

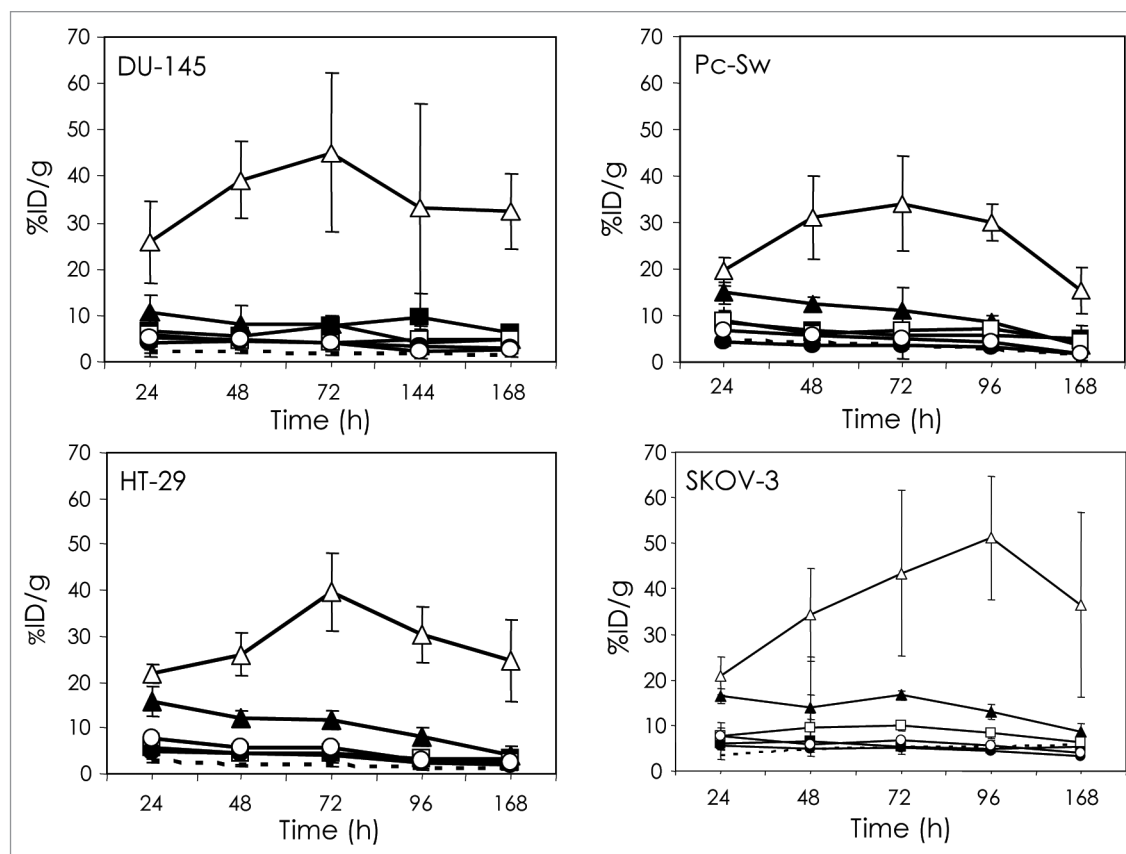


Figure 3. Tumor and normal tissue distribution of ^{111}In -trastuzumab. Athymic mice bearing human of prostate (DU-145), pancreatic (PC-Sw), ovarian (SKOV-3) and colon (HT-29) carcinoma tumors were injected i.v. with ^{111}In -trastuzumab ($\sim 7.5 \mu\text{Ci}/2.3 \mu\text{g}$ trastuzumab) when the tumors were 0.4–0.6 cm in diameter and euthanized at the indicated time points. Blood (closed triangle), tumor (open triangle), liver (closed square), spleen (open square), kidneys (closed circle), lungs (open circle) and femur (dotted line) were harvested, wet-weighted and counted in a γ -counter. The %ID/g were calculated and plotted along with the standard deviations.

Table 3. Tumor and tissue distribution of ^{111}In -trastuzumab in athymic mice bearing s.c. xenografts of human prostate (PC3) carcinoma cells

| Tissue | Time points (h) | | | | |
|------------------|-----------------|--------------|---------------|--------------|--------------|
| | 24 | 48 | 72 | 120 | 168 |
| Blood | 11.89 (2.25) | 7.77 (4.43) | 9.12 (3.12) | 9.08 (1.32) | 6.36 (2.57) |
| Tumor | 13.40 (4.44) | 11.65 (4.12) | 23.62 (15.24) | 20.64 (7.96) | 19.22 (7.40) |
| Liver | 3.65 (1.08) | 3.44 (0.59) | 4.77 (1.77) | 3.44 (0.41) | 3.37 (0.65) |
| Spleen | 3.59 (0.90) | 2.77 (0.94) | 3.46 (1.29) | 4.34 (0.71) | 4.16 (1.71) |
| Kidneys | 4.07 (0.41) | 3.04 (1.00) | 3.21 (1.06) | 3.01 (0.35) | 2.07 (0.52) |
| Lungs | 8.82 (8.04) | 3.89 (1.88) | 4.66 (1.71) | 4.69 (0.85) | 3.10 (1.02) |
| Heart | 3.70 (0.54) | 2.91 (1.79) | 2.68 (0.76) | 2.50 (0.43) | 2.24 (0.82) |
| Stomach | 1.60 (0.42) | 1.29 (0.64) | 1.44 (0.39) | 1.47 (0.28) | 1.18 (0.32) |
| Small Intestine | 1.54 (0.46) | 1.24 (0.43) | 1.56 (0.41) | 1.37 (0.09) | 1.20 (0.45) |
| Large Intestine | 1.24 (0.40) | 1.14 (0.54) | 1.23 (0.31) | 1.33 (0.18) | 1.12 (0.47) |
| Testes | 1.94 (0.52) | 1.84 (0.49) | 2.08 (0.55) | 2.08 (0.52) | 2.05 (0.64) |
| Vesicular Glands | 0.67 (0.19) | 0.75 (0.36) | 0.79 (0.23) | 0.70 (0.15) | 0.86 (0.47) |
| Urinary Bladder | 2.86 (1.01) | 2.02 (0.52) | 3.28 (1.44) | 3.84 (2.00) | 2.18 (0.58) |
| Femur | 1.69 (0.46) | 1.43 (0.44) | 1.60 (0.46) | 1.47 (0.91) | 1.45 (0.43) |

*Athymic mice bearing s.c. PC-3 xenografts (0.4–0.6 cm in diameter) were injected (i.v.) with ^{111}In -trastuzumab ($\sim 7.5 \mu\text{Ci}/2.3 \mu\text{g}$ trastuzumab). The mice were sacrificed by exsanguination, the blood and tissues were harvested, wet-weighted and the radioactivity measured. The values represent the average percent injected dose per gram of tissue (%ID/g). The standard deviations were also calculated and are given in parentheses.

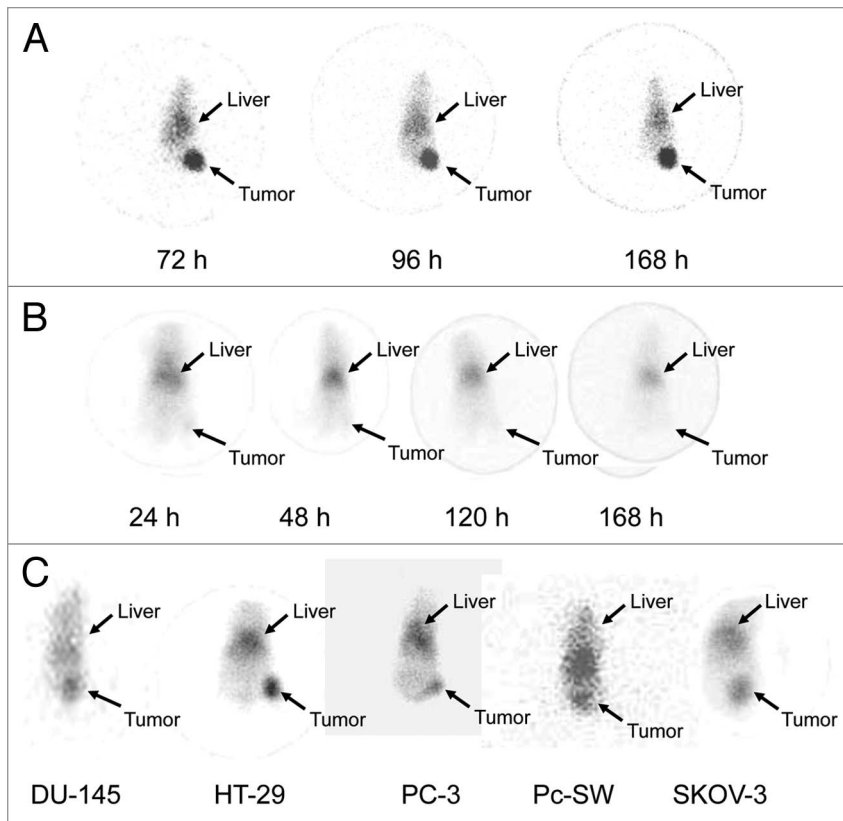


Figure 4. Scintigraphic analysis of athymic mice following i.v. injection of ^{111}In -trastuzumab. Mice bearing HER2-positive s.c. LS-174T (0.4–0.6 cm diameter) (A) or HER2-negative s.c. melanoma (A375) xenografts (B) were given i.v. injections of ^{111}In -CHX-A'-trastuzumab (~80–100 μCi /1.0–1.3 μg trastuzumab) and γ -scintigraphy performed over a one week period. Mice bearing s.c. xenografts of human prostate (DU-145, PC3), pancreas (PC-Sw), ovarian (SKOV-3) and colon (HT-29) carcinoma were also injected with ^{111}In -CHX-A'-trastuzumab and imaged. The images acquired at 72 h are presented for comparative purposes (C).

23.62 ± 15.24 at 72 h. The peak %ID/g for the HT-29, PC-Sw and DU-145 tumors was 39.67 ± 8.50 , 34.00 ± 10.15 and 45.06 ± 7.22 at 72 h.

Among these five tumor models, the biodistribution of the RIC to the normal organs demonstrated similar levels and patterns. In general, the highest level (%ID/g) was observed at 24 h, with a decreasing trend through 168 h of the experiment. Levels found in the spleens and femurs from the mice bearing the SKOV-3 xenografts were exceptions. Not only does the spleen from these animals result in a higher %ID/g, the peak value is found at 72 h. Regarding the femurs, there is a modest increasing trend in the uptake of the RIC.

A prostate carcinoma model (PC-3) was selected for a more extensive evaluation of the RIC in male mice (Table 3). The biodistribution pattern of the RIC proved to be similar to that of the other tumor models using female mice. The highest tumor %ID/g (23.62 ± 15.24) was obtained 72 h post-injection of the ^{111}In -trastuzumab. With the exception of blood and the lungs at 24 h, all other normal tissues had %ID/g values less than 5. Uptake in organs such as the testes and vesicular glands was unremarkable.

Targeting of HER2 for planar γ -scintigraphy and positron-emission tomography of i.v. injected radiolabeled trastuzumab. Tumor targeting and the potential of ^{111}In -trastuzumab for imaging were demonstrated by two imaging modalities, γ -scintigraphy and PET. As depicted in Figure 4A, localization of the RIC in the s.c. LS-174T xenograft on the rear flank of the mouse was clearly evident by γ -scintigraphy at 72 h, with some activity present in the heart, lungs and liver. This activity was found to persist in the tumor through the 96 and 168 h time points while the background signal (heart, lungs and liver) decreased. Specificity of the ^{111}In -trastuzumab was demonstrated in mice bearing the s.c. A375 (melanoma) xenografts injected with the RIC; γ -scintigraphic images were taken over the course of a week (Fig. 4B). Consistent with the biodistribution data already discussed, most of the radioactivity was observed in the heart, lungs and liver, suggestive of the presence of the RIC in the blood compartment. In contrast, the irrelevant A375 tumor xenograft was not visible.

γ -Scintigraphy was also performed with each of the previously noted tumor models to demonstrate the applicability of ^{111}In -trastuzumab for potential management and therapy of patients with a range of cancers. Images of each tumor model were collected over a 168 h period; the 72 h images were selected for comparison to the images taken of the LS-174T model (Fig. 4C). In each of the models, there was targeting of the tumor xenograft, which provided tumor visualization and supported the quantitative analysis of the data discussed.

The LS-174T (s.c.) tumor xenografts were clearly visualized by PET imaging, which was performed with ^{86}Y -labeled trastuzumab. No significant background following i.v. administration of ^{86}Y -trastuzumab (Fig. 5A) was evident by 72 h. Upon completion of the 72 h imaging session, the mice were euthanized and analysis of the biodistribution of ^{86}Y -labeled trastuzumab was performed. The tumor uptake values determined by direct analysis of the tissues and quantitative PET were identical ($p = 0.94$, $n = 6$).

Targeting and detection of disseminated peritoneal disease using radiolabeled trastuzumab. The ability to effectively target disseminated peritoneal disease with locoregional administration of ^{111}In -trastuzumab was investigated in an i.p. model with the LS-174T tumor. ^{111}In -trastuzumab (~7.5 μCi) was administered via i.p. injection to mice bearing 5 d peritoneal LS-174T xenografts. Over the period of 1 week, tumor and normal tissues were collected for analysis. Excellent tumor targeting was obtained, with a %ID/g as high as 130.85 ± 273.34 at 24 h (Table 4). Tumor masses, ranging from 3–177 mg (25.6 ± 35.0 mg), were harvested from multiple sites throughout the peritoneum. The

tumor was typically associated with and adherent to, liver, spleen, pancreas, walls of the peritoneum and fat in the pelvic region. The %ID/g remained high at 48, 72 and 96 h, with values of 66.77 ± 58.88 , 43.78 ± 24.64 and 43.57 ± 24.52 , respectively. At the 168 h time point, the tumor burden ranged from 7–1,058 (128.5 ± 205.6 mg), with a %ID/g of 14.8 ± 12.3 ; this lower value most likely reflected the increase in tumor burden. Greater involvement of tumor with normal tissues determined by macroscopic examination was evident. Among the normal organs (Table 4), the ovaries, gall bladder, spleen, pancreas, uterus and urinary bladder presented with high %ID/g values, with the highest %ID/g of 40.98 ± 53.32 for the ovaries observed at 24 h. In this circumstance, the high value is attributable to one animal for which the ovary %ID/g was 135.9. This is most likely due to the presence of tumor that could not be visually discriminated and dissected. The values for the other four tumor-bearing mice in this group were 18.08, 9.08, 23.67 and 16.16. In this same animal, high uptake of the RIC also occurred in the gall bladder; the %ID/g was 112.68, while the values calculated for the other animals were 16.8 or less.

Because a higher uptake of the RIC in the normal organs was observed, a study was conducted to assess the distribution of i.p. administered ^{111}In -trastuzumab in non-tumor-bearing animals. The high %ID/g values cited above were not observed in the organs collected from mice in which tumor was absent (Table 4). In general, the level of RIC uptake in the normal organs of the tumor-bearing mice was comparable to the uptake in the organs of non-tumor-bearing mice that had received ^{111}In -trastuzumab by i.v. injection. For the organs such as the ovaries, gall bladder, pancreas, lymph nodes and stomach, there were only one or two time points for each of these organs that have higher %ID/g values than the tumor-bearing mice, while the rest of the time points were comparable to the levels observed in the non-tumor-bearing mice.

Blood pharmacokinetics of i.p. injected ^{111}In -trastuzumab. Mice bearing i.p. tumor (LS-174T) xenografts and non-tumor-bearing mice were injected i.p. with ^{111}In -trastuzumab ($-7.5 \mu\text{Ci}/2.3 \mu\text{g}$ trastuzumab). Differences between the two groups of mice were immediately apparent. Appearance of ^{111}In -trastuzumab in the blood from the peritoneum of non-tumor-bearing mice peaked at 2 h and exhibited a bi-exponential clearance from the blood. In the tumor-bearing mice, the egress of the RIC from the peritoneum into the circulation peaked 4 h post-injection. The relationship of the clearance rates in the non-tumor vs. the tumor-bearing mice was the same as the i.v. injected groups of mice. The $T_{1/2\alpha}$ and $T_{1/2\beta}$ values are 4-fold and 2-fold greater, respectively, in the non-tumor-bearing mice vs. the tumor-bearing mice (Table 2).

Planar γ -scintigraphy and positron-emission tomography of disseminated intraperitoneal disease. Treatment of disseminated peritoneal disease with trastuzumab radiolabeled with α -particle emitters is a primary focus of studies within this laboratory. As such, monitoring of disease and response to therapy would prove a useful tool for optimizing a treatment regimen. Such a capability would also prove beneficial in the pending clinical study at the University of Alabama for monitoring ovarian cancer patients

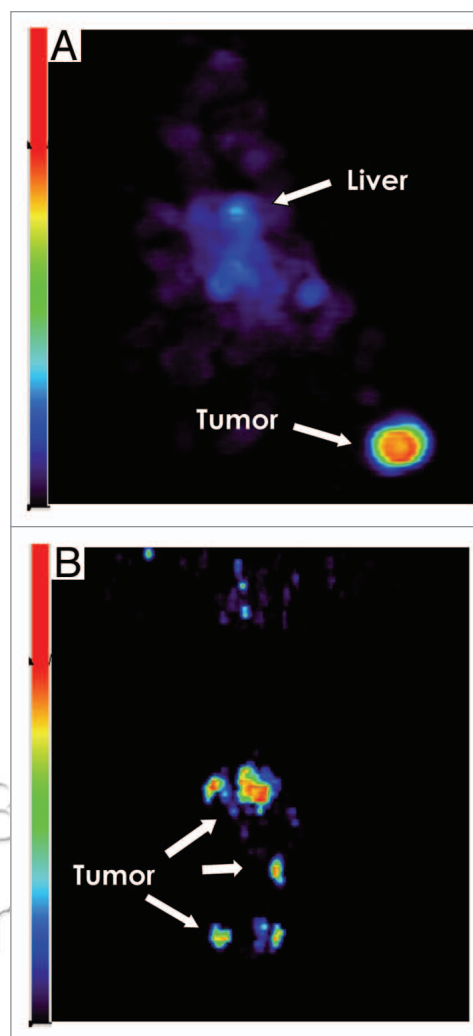


Figure 5. Representative reconstructed and processed maximum intensity whole body projections from positron emission tomography (PET) of athymic mice bearing tumor xenografts injected with ^{86}Y -CHX- A^2 -trastuzumab. Mice bearing s.c. (A) and i.p. (B) LS-174T xenografts were given i.v. or i.p. injections, respectively, of ^{86}Y -trastuzumab ($80\text{--}100 \mu\text{Ci}/4.3\text{--}5.3 \mu\text{g}$ trastuzumab) and imaged 3-D post-injection of the radioimmunoconjugate. The location of the liver and tumor(s) are

following radioimmunotherapy with ^{212}Pb -trastuzumab. With this in mind, mice bearing i.p. LS-174T tumors were injected (i.p.) with $80\text{--}100 \mu\text{Ci}$ ($1\text{--}1.3 \mu\text{g}$) of ^{111}In -trastuzumab and imaged at 24, 48, 72 and 144 h. Forty-eight hours post-injection with RIC, masses were evident in the peritoneum by γ -scintigraphy (Fig. 6A). As unbound RIC cleared from the peritoneum or further targeting occurred, the masses became more distinct at the 72 h and 144 h time points, while negligible activity was observed in the rest of the mouse. The mice were euthanized at 144 h due to progression of disease, the macroscopic tumor was collected and the %ID/g determined. Tumor masses, from the mouse presented in Figure 6A were excised from between the liver lobes, top of the stomach, adherent to the spleen, pancreas, ovaries and from the abdominal wall with %ID/g of 25, 18.1, 22.1, 20.8, 13.3 and 14.6, respectively. When non-tumor-bearing mice were given

Table 4. Tumor targeting and normal organ distribution of ¹¹¹In-trastuzumab following i.p. administration in athymic mice, non-tumor-bearing and bearing i.p. LS-174T xenografts

| Non-tumor-bearing mice | | | | | |
|------------------------|-----------------|---------------|---------------|---------------|---------------|
| Tissue | Time points (h) | | | | |
| | 24 | 48 | 72 | 96 | 168 |
| Blood | 12.73 (4.20) | 10.02 (7.09) | 7.75 (4.58) | 8.76 (3.39) | 1.95 (0.30) |
| Brain | 0.43 (0.15) | 0.34 (0.19) | 0.26 (0.12) | 0.27 (0.08) | 0.07 (0.01) |
| Liver | 5.06 (1.21) | 7.71 (4.06) | 5.33 (0.43) | 6.36 (0.84) | 1.15 (0.23) |
| Spleen | 5.97 (1.11) | 8.96 (3.21) | 7.32 (1.27) | 9.05 (1.44) | 1.99 (0.22) |
| Kidneys | 5.92 (1.25) | 5.47 (1.01) | 4.27 (1.06) | 5.02 (0.89) | 1.25 (0.44) |
| Lungs | 6.25 (2.24) | 4.82 (2.10) | 4.17 (2.04) | 4.88 (1.74) | 1.14 (0.40) |
| Heart | 4.46 (0.98) | 4.25 (1.23) | 3.28 (1.67) | 3.41 (1.43) | 0.88 (0.32) |
| Stomach | 2.04 (0.21) | 3.06 (0.68) | 1.80 (0.22) | 2.05 (0.29) | 0.38 (0.08) |
| Small Intestine | 2.24 (0.27) | 2.89 (0.93) | 2.35 (0.71) | 2.30 (0.30) | 0.34 (0.07) |
| Large Intestine | 2.03 (0.39) | 2.65 (0.82) | 2.14 (0.64) | 2.13 (0.36) | 0.33 (0.03) |
| Ovaries | 2.83 (0.61) | 4.56 (1.59) | 3.05 (1.80) | 2.53 (1.33) | 0.62 (0.20) |
| Uterus | 4.18 (1.11) | 7.16 (3.91) | 7.22 (3.81) | 6.25 (2.42) | 1.13 (0.26) |
| Urinary Bladder | 4.29 (1.82) | 5.15 (2.80) | 2.70 (0.86) | 2.48 (0.62) | 0.59 (0.23) |
| Muscle | 1.81 (0.46) | 1.30 (0.44) | 0.98 (0.45) | 0.87 (0.12) | 0.28 (0.10) |
| Skin | 5.30 (1.22) | 6.08 (1.03) | 4.57 (1.73) | 3.37 (1.11) | 0.73 (0.18) |
| Axillary Lymph Node | 3.22 (1.58) | 4.56 (2.58) | 4.44 (1.35) | 1.96 (0.34) | 0.78 (0.14) |
| Femur | 3.31 (0.43) | 6.27 (1.80) | 4.64 (2.87) | 5.19 (2.16) | 2.07 (1.11) |
| Gall Bladder | 1.28 (0.49) | 2.95 (2.21) | 3.69 (2.75) | 1.86 (1.06) | 0.45 (0.35) |
| Thyroid | 3.25 (0.68) | 4.25 (0.85) | 3.04 (0.51) | 3.70 (1.05) | 0.63 (0.20) |
| Pancreas | 4.62 (0.93) | 6.74 (4.09) | 5.66 (1.50) | 5.30 (1.54) | 1.14 (0.12) |
| Tumor-bearing mice | | | | | |
| Tissue | Time points (h) | | | | |
| | 24 | 48 | 72 | 96 | 168 |
| Blood | 17.51 (3.05) | 11.77 (8.06) | 6.24 (5.56) | 4.33 (2.93) | 1.07 (1.08) |
| Tumor | 130.85 (273.34) | 66.77 (58.89) | 43.78 (21.64) | 43.57 (24.52) | 14.81 (12.31) |
| Brain | 0.48 (0.09) | 0.30 (0.16) | 0.17 (0.12) | 0.15 (0.07) | 0.07 (0.03) |
| Liver | 6.97 (1.85) | 5.19 (1.78) | 5.42 (3.83) | 4.43 (1.38) | 2.63 (1.08) |
| Spleen | 13.26 (7.01) | 8.28 (3.24) | 8.67 (6.05) | 7.89 (3.05) | 4.93 (2.84) |
| Kidneys | 6.57 (1.07) | 5.06 (2.23) | 3.78 (1.83) | 3.87 (0.99) | 2.42 (0.63) |
| Lungs | 7.56 (1.25) | 5.19 (2.92) | 3.24 (2.56) | 2.67 (1.20) | 1.04 (0.47) |
| Heart | 5.32 (1.00) | 3.42 (2.05) | 2.39 (1.71) | 1.74 (0.76) | 0.62 (0.28) |
| Stomach | 4.55 (1.94) | 2.90 (1.16) | 2.73 (1.19) | 3.51 (2.54) | 0.97 (0.56) |
| Small Intestine | 3.70 (1.43) | 2.61 (1.08) | 2.49 (1.29) | 1.88 (0.69) | 1.01 (0.39) |
| Large Intestine | 3.10 (0.72) | 2.24 (0.88) | 1.46 (0.80) | 1.58 (0.55) | 0.74 (0.12) |
| Ovaries | 40.98 (53.32) | 8.82 (7.10) | 5.00 (1.42) | 5.11 (2.39) | 3.71 (3.57) |
| Uterus | 9.93 (7.17) | 7.73 (2.60) | 5.57 (2.26) | 5.46 (1.76) | 3.04 (2.21) |
| Bladder | 11.55 (9.77) | 4.87 (2.18) | 2.44 (1.09) | 2.95 (0.65) | 1.37 (0.45) |
| Muscle | 1.69 (0.95) | 1.23 (0.50) | 1.24 (0.97) | 0.71 (0.32) | 0.44 (0.19) |
| Skin | 5.43 (1.87) | 6.34 (5.21) | 2.69 (1.32) | 2.74 (0.25) | 1.46 (0.50) |
| Axillary Lymph Node | 12.09 (4.74) | 19.64 (26.11) | 6.55 (1.72) | 7.12 (2.47) | 5.88 (4.58) |
| Femur | 3.19 (1.18) | 3.81 (1.69) | 3.38 (1.51) | 3.69 (0.82) | 2.58 (0.77) |
| Gall Bladder | 34.60 (52.39) | 5.11 (4.44) | 21.70 (18.84) | 21.85 (9.74) | 6.37 (5.47) |

^aAthymic mice bearing s.c. LS-174T xenografts and non-tumor bearing mice were injected (i.p.) with ¹¹¹In-trastuzumab (~7.5 μCi/2.3 μg trastuzumab). The mice were sacrificed by exsanguination, the blood and tissues were harvested, wet-weighted and the radioactivity measured. The values represent the average percent injected dose per gram of tissue (%ID/g). The standard deviations were also calculated and are given in parentheses.

Table 4. Tumor targeting and normal organ distribution of ^{111}In -trastuzumab following i.p. administration in athymic mice, non-tumor-bearing and bearing i.p. LS-174T xenografts

| | | | | | |
|----------|--------------|---------------|-------------|-------------|-------------|
| Thyroid | 9.81 (14.01) | 2.74 (1.48) | 1.61 (0.77) | 2.11 (0.65) | 1.08 (0.25) |
| Pancreas | 8.91 (5.65) | 16.81 (17.32) | 7.71 (4.77) | 5.51 (3.60) | 3.78 (3.44) |

^aAthymic mice bearing s.c. LS-174T xenografts and non-tumor bearing mice were injected (i.p.) with ^{111}In -trastuzumab (~7.5 μCi /2.3 μg trastuzumab). The mice were sacrificed by exsanguination, the blood and tissues were harvested, wet-weighted and the radioactivity measured. The values represent the average percent injected dose per gram of tissue (%ID/g). The standard deviations were also calculated and are given in parentheses.

^{111}In -trastuzumab i.p., there was persistence of activity in the region of the heart, lungs and liver (Fig. 6B), particularly so when compared to what was observed with tumor-bearing mice at 144 h.

Visualization of LS-174T tumor masses in the peritoneum was also accomplished with PET imaging when ^{86}Y -trastuzumab was administered by i.p. injection (Fig. 5B). Location of the tumor masses was similar to what was found in the mice from the planar γ -scintigraphic study, as well as what was observed during the biodistribution study. Due to the inherent limitations of small animal PET for imaging small lesions, absolute quantitative correlation was not achieved between PET and biodistribution studies ($p = 0.002$); however, when tumor to liver ratios were used, relative quantitative correlation was achieved as the values determined from PET and biodistribution were similar ($p = 0.91$).

Effect of trastuzumab amount on tumor targeting. Finally, an experiment was designed to determine the influence of the specific activity (mCi/mg) of ^{111}In -trastuzumab on tumor targeting. HER2 is an internalizing target and the loss of this receptor from the cell surface could have an impact on the overall amount of radiolabeled trastuzumab binding to the cells or tumor mass. This is certainly a consideration when using a RIC for the delivery of therapeutic doses of a radionuclide. Trastuzumab was radiolabeled at a high specific activity (82–93 mCi/mg) and then diluted with unlabeled trastuzumab. Mice ($n = 5$) with s.c. LS-174T tumor xenografts were then injected i.v. with 4.0 μCi of ^{111}In -trastuzumab containing 0.05–200 μg of unlabeled trastuzumab, euthanized 72 h later, the tissues collected and the %ID/g calculated. Previous studies from this laboratory have demonstrated that 300 μg of trastuzumab does not prolong the survival of mice with i.p. xenografts of the LS-174T tumor cell line.¹³ The study compared animals bearing large tumors (1,057 \pm 520 mg) to those with a lesser tumor burden (257 \pm 102 mg). Beginning with the smaller tumor burden (Fig. 7A), the 3 lower doses of trastuzumab resulted in comparable tumor %ID/g values, 35.8 \pm 10.2, 35.0 \pm 6.6 and 40.5 \pm 5.7 at 0.05, 0.1 and 10 μg , respectively. There is a noticeable decrease in the %ID/g of the tumor starting with 17.1 \pm 2.2 at the 25 μg dose and ending with 8.85 \pm 1.1 at the 200 μg

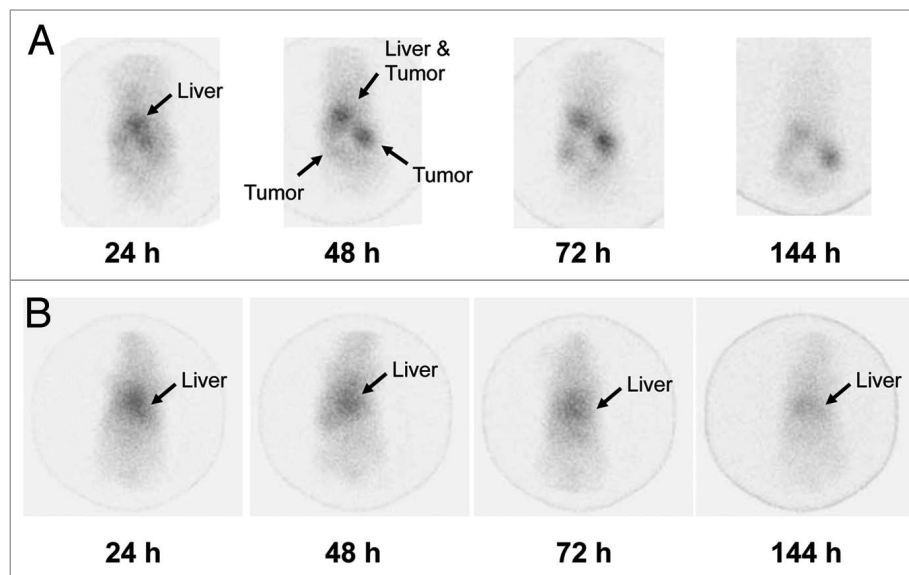


Figure 6. Scintigraphic analysis of athymic mice following i.p. injection of ^{111}In -trastuzumab. Mice bearing i.p. LS-174T xenografts (A) or non-tumor-bearing mice (B) were given i.p. injections of ^{111}In -CHX-A'-trastuzumab (~80–100 μCi /1.0–1.3 μg trastuzumab) and γ -scintigraphy performed over a one week period. The location of the liver and tumor(s) are indicated.

dose of trastuzumab. No differences were discerned in the normal organs. Shown in Figure 7B, a similar pattern was observed when the same experiment was performed with mice bearing a larger tumor burden. At the two lower doses (0.05 and 10 μg) of trastuzumab, similar %ID/g were obtained for the tumors (25.8 \pm 4.8 and 22.1 \pm 3.6). The tumor %ID/g then declined from 16.7 \pm 0.2 for the 25 μg dose to 8.1 \pm 3.2 for the 200 μg dose. Again, no differences were apparent among the normal organs.

Discussion

HER2, a member of the epidermal growth factor receptor family, is overexpressed by a wide variety of epithelial cancers compared to normal tissues.^{30–33} In fact, overexpression of HER2 is associated with aggressive disease as well as metastatic disease.³⁴ The differential in HER2 expression between normal and malignant tissues has been sufficient to provide a molecular target for therapies, including small molecules such as 17-allylaminogel-danamycin (17-AAG) and large molecules such as trastuzumab (Herceptin®).³ In fact, the prospects of trastuzumab for the treatment of breast cancer were so promising that in 1998 it became the first humanized mAb to be approved by the FDA. Since

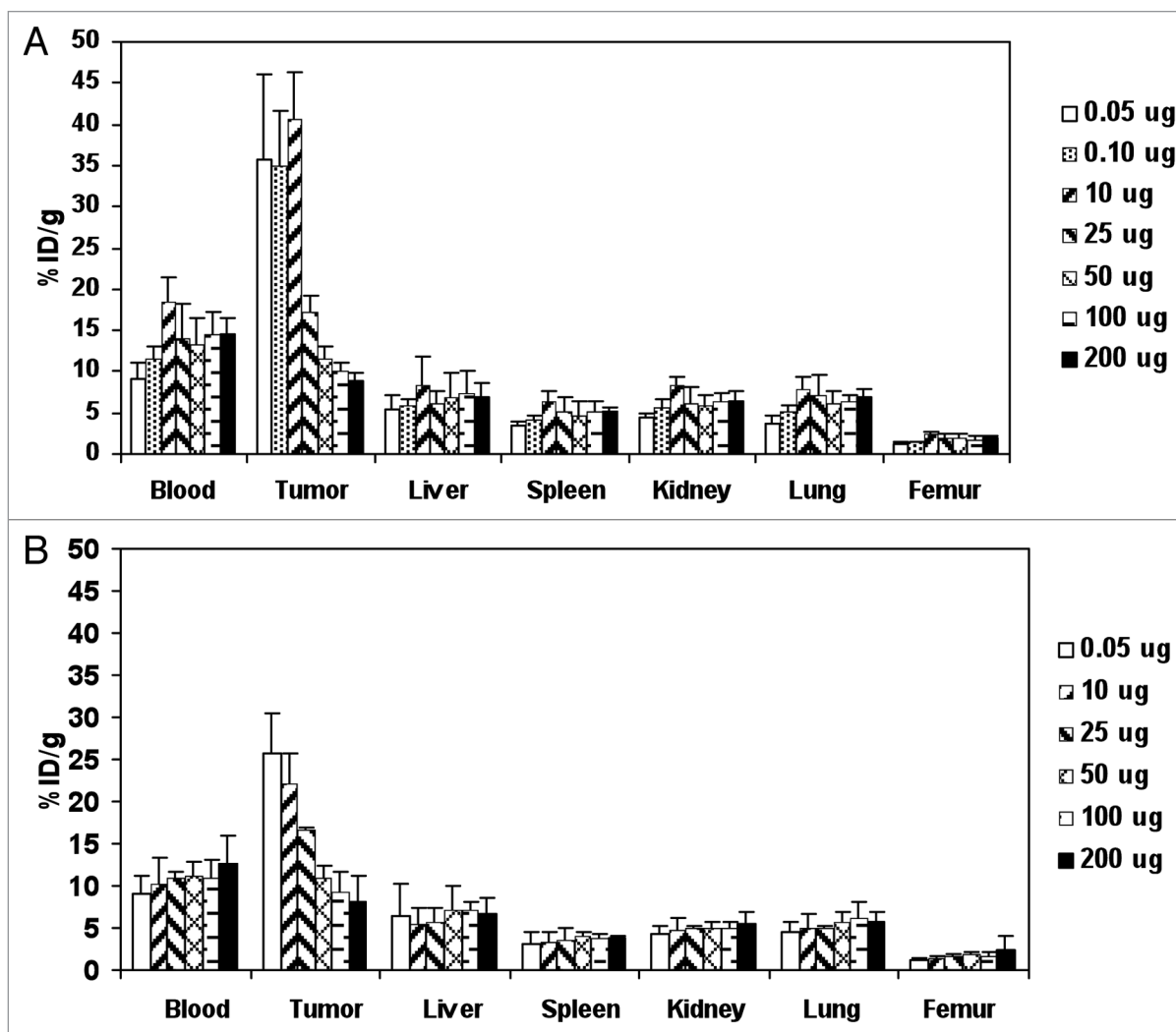


Figure 7. Effect of specific activity on the tumor targeting of $^{111}\text{In-CHX-A''-trastuzumab}$. Mice ($n = 5$) bearing s.c. LS-174T xenografts were injected with $^{111}\text{In-CHX-A''-trastuzumab}$ ($\sim 7.5 \mu\text{Ci}$) containing 0.05 to 200 μg of trastuzumab. Mice ($n = 5$) were euthanized at 72 h, blood, tumor and organs were harvested, wet-weighted and the radioactivity measured. The %ID/g with the standard deviations was plotted. A comparison of small tumor burden ($257 \pm 102 \text{ mg}$) in (A) to a larger tumor burden ($1,057 \pm 520 \text{ mg}$) in (B) is presented.

then, the limitations of trastuzumab as a monotherapy have become well-documented.^{3,5} Pre-clinical and clinical studies from this laboratory and others, however, have demonstrated the feasibility of targeting HER2 with trastuzumab conjugated with medically relevant radionuclides.^{11-15,17,19,21,26,35-37} When radiolabeled with α - or β -particle emitting radionuclides, trastuzumab has been efficacious in increasing the median survival of tumor-bearing mice.^{11,13,15,16,19,37} Meanwhile, trastuzumab labeled with radionuclides possessing γ - or β^+ -emissions, is being investigated to detect HER2 tumor expression as a means of selecting patients for HER2 therapy or monitoring patients during those treatments.^{18,21,24,25,27-29} Information such as this would allow the clinician to assess the benefit of the therapy, and if there is treatment failure, to then modify the patient's treatment regimen. In the case of patients receiving trastuzumab therapy, imaging may also serve as a means to identify patients at risk for myocardiotoxicity.^{12,20,26} More specific to RIT with trastuzumab,

imaging can provide information for dosimetric calculations/predictions.¹⁷

Trastuzumab has proven to be a rather robust mAb that well-tolerates modification with three to four chelates without loss of immunoreactivity, which is comparable to results reported by other investigators.^{12,18,19,29} For example, four to five DOTA ligands have been added to trastuzumab without any deleterious results, and Reilly et al. have reported the modification of trastuzumab Fab fragment with two to three molecules of the DTPA anhydride chelate.^{18,19,29} One group reported aggregate formation if the conjugation reaction of DTPA anhydride to trastuzumab exceeded a molar excess of 1:1; they did not report the actual number of chelates that were conjugated to trastuzumab.¹² The data provided in the present report indicates that trastuzumab radiolabeled with ^{111}In retains its reactivity with HER2 expressing cells even with specific activities as high as 177 mCi/mg. The ability to attain high specific activity and still retain

immunoreactivity is an important consideration in the design of radioimmunotherapy trials in which higher doses are required. Also relevant is the need to understand how the total amount of protein in the dose influences the targeting and trafficking of the radioimmunoconjugate.

The choice of CHX-A^{99m}Tc-DTPA as the chelating component of the trastuzumab conjugate was dictated by two factors. First, CHX-A^{99m}Tc-DTPA has been conjugated to mAbs such as HuS193 and HuM195 and used in clinical studies.³⁸⁻⁴¹ Second, GMP production and the requisite testing of a conjugated mAb is an expensive venture both in money and time. CHX-A^{99m}Tc-DTPA has been found to be a suitable ligand for radiolabeling mAbs with ¹⁷⁷Lu, ²¹³Bi, ²¹²Bi, ⁸⁶Y and ¹¹¹In.^{22,42-44} Reaction of CHX-A^{99m}Tc-DTPA with each of these radionuclides provides for efficient radiolabeling that can be accomplished in a short period of time at temperatures, i.e., 37°C, appropriate for proteins. Thus, one immunoconjugate that has the potential to be utilized in an array of either imaging or RIT applications can be produced.

Excellent tumor targeting of the ¹¹¹In-CHX-A^{99m}Tc-DTPA-trastuzumab was obtained in each of the xenograft models evaluated, with peak %ID/g values occurring at 48–72 h. In general, the values are presented here are in agreement with previous reports that reported targeting of breast cancer xenografts.^{11,19,24} In the studies presented here, an ovarian (SKOV-3) and prostate (DU-145) carcinoma xenograft, resulted in the greatest uptake of the radioimmunoconjugate. Interestingly, targeting of SKOV-3 xenografts has been presented previously and the peak tumor %ID/g obtained was 16.3, one-third of what is reported here.¹² The poorer tumor targeting may be a reflection of the stability or quality of the radiolabeled trastuzumab conjugate that was injected. The investigators state that 7% of the radioactivity was lost, daily, from the radioimmunoconjugate. Specificity of the ¹¹¹In-CHX-DTPA-trastuzumab was demonstrated using a HER2-negative tumor xenograft model, as well as by injecting mice bearing HER2 positive tumors with an ¹¹¹In-labeled non-specific antibody.

Not only was tumor targeting obtained in each of the models investigated, a lack of uptake by the normal tissues was observed. In the absence of HER2-positive tumor, the level of radioactivity was higher in the blood and normal organs. This observation was confirmed by the pharmacokinetic studies. In the absence of an antigen sink, i.e., the HER2-positive tumor, the RIC was found to persist in the blood compartment. When the RIC was given by i.v. administration, both the T_{1/2}α- and β-phases were 2- and 2.8-fold greater, respectively, in the non-tumor-bearing mice vs. the tumor-bearing mice. The data suggests that the tumor is more than likely facilitating the rapid clearance of the RIC from the blood. Similar differences were also noted in the groups of mice that received the ¹¹¹In-CHX-DTPA-trastuzumab by i.p. injection. Since the cognate antigen of trastuzumab is human HER2, then the only source of HER2 is the tumor. Trastuzumab does not recognize murine HER2 in the tissues or circulating in the blood.

In 2008, a report from this laboratory noted a similar clearance pattern for ¹¹¹In-labeled cetuximab.⁴⁵ In contrast, the bi-exponential clearance of ¹¹¹In-panitumumab proved to be the

reverse of that observed for cetuximab and trastuzumab.⁴⁶ It is unclear at this time if the clearance rates are influenced more by the target antigen, i.e., degree and rate of internalization, the mAb affinity for the antigen, the mAb isotype, the form of the mAb (panitumumab is fully human) or a combination of all of the above.

Also noteworthy is the observation that the amount of ¹¹¹In-CHX-DTPA-trastuzumab in the blood does not appear to be influenced by the amount of tumor burden. In the study assessing the effect of specific activity on tumor targeting (Fig. 7), mice with a tumor burden of 257 ± 102 mg presented with the same blood %ID/g (9.16 ± 3.33) as mice with a tumor burden of 1,057 ± 520 mg (9.13 ± 3.00).

The highest uptake of the ¹¹¹In-trastuzumab was observed with i.p. administration of the RIC to target i.p. xenografts, thus strengthening the argument that locoregional treatment of disease might be an optimal application.^{47,48} Additional studies comparing i.p. vs. i.v. injection of ¹¹¹In-trastuzumab for the targeting of tumors at different sites (s.c., i.p., intrathoracic) is warranted. The LS-174T tumor model is quite aggressive and mice with i.p. tumors routinely succumb to disease in ~three weeks; the tumor burden disseminates throughout the peritoneum. It is not unexpected then for the normal tissues of the peritoneum to exhibit a higher %ID/g than what was obtained in the non-tumor-bearing mice and, as with ovarian and pancreatic cancer patients, removal of the entire tumor burden is not entirely possible. The higher %ID/g of some of the normal tissues most likely results from the presence of some tumor tissue. This issue will be revisited in upcoming experiments in which the tissues will be appropriately handled and processed for histochemical examination.

The ability to image both the s.c. and i.p. xenografts by planar γ-scintigraphy and PET further validates the clinical potential of radiolabeled CHX-A^{99m}Tc-DTPA-trastuzumab for the treatment and management of a patient population beyond breast cancer. Imaging will provide much needed information for the dosimetry of trastuzumab in RIT applications, a requisite for the responsible administration of radiolabeled mAb used for therapy. Several groups have evaluated trastuzumab as an imaging agent with various levels of success.^{12,17,21,25,29,49} Sgouros and colleagues have reported using a peritoneal model of disseminated ovarian cancer in which microPET image intensity in the tumor matched the tumor uptake of radioactivity that was quantitated by direct tissue analysis.¹⁷ They also demonstrated that the dosimetry calculations were strongly influenced by the size of the tumor determined by combining microPET images with MRI.

As a prelude to the clinical trials, the influence of specific activity on tumor targeting was evaluated in mice with s.c. LS-174T tumor xenografts. Depletion of this receptor from the cell surface with the binding of radiolabeled trastuzumab could affect the overall amount of radiolabeled trastuzumab binding to the cells or tumor mass and certainly the therapeutic dose in RIT regimens. If high specific activities can be achieved with a radioimmunoconjugate, then the amount of antibody may be minimized. If, for whatever reason, a RIC is injected at low specific activities, i.e., poor labeling efficiency or prevention of radiolysis, then it is important to understand how tumor targeting is affected

by the higher levels of the mAb. Decreased tumor targeting was observed with increasing doses of trastuzumab or lower specific activity. In contrast, a recent clinical study by Dijkers et al. demonstrated that lower specific activity of ^{89}Zr -trastuzumab actually provided better scans by PET imaging.⁵⁰ Patients on trastuzumab therapy required a 10 mg dose of trastuzumab for optimal tumor visualization, while trastuzumab-naïve patients required a higher dosage (50 mg) of the mAb. This dichotomy may reflect limitations of the mouse model employed and the specificity of trastuzumab for human HER2. Trastuzumab does not react with murine HER2 present in normal tissues and therefore saturation of the target antigen in normal tissues is a moot issue. The study by Dijkers et al. also highlights another limitation of the murine model.⁵⁰ In the studies presented here, optimal targeting of the ^{111}In -trastuzumab occurred 48–72 h post-injection in four of the five tumor xenograft models evaluated. In contrast, the optimal visualization ^{89}Zr -trastuzumab in patients was found to occur at 96–120 hrs.⁵⁰ This discrepancy is most likely the result of injecting mice with a xenogenic (human) mAb.

In the arena of monitoring patients during a treatment regimen, trastuzumab radiolabeled with ^{64}Cu has been explored as a tool for PET imaging of HER2 expression as an indicator of tumor responsiveness to Hsp90 inhibitors.²⁵ Trastuzumab F(ab')₂ fragments radiolabeled with ^{68}Ga have been investigated for this same purpose as have genetically engineered forms such as diabodies and affibodies.^{27,51,52} In fact, the on-going clinical study NCT00613847 with ^{68}Ga -trastuzumab at Memorial Sloan Kettering Cancer Center is assessing its potential for PET imaging patients with solid tumors that are HER2-positive.

Trastuzumab is also being investigated for optical imaging.^{53,54} Signal attenuation in tissues, however, abrogates the ability to quantify an agent with an optical probe. One solution to this problem is to create a dual-labeled agent, one label being the optical dye and the other being a radionuclide.^{53,55} One strategy to achieve this goal is to conjugate the targeting vector with the optical dye and radioactivity, either as a dual modification or as a single modification, and then make a “cocktail” containing the separate optical and radioactive probes.

The limitations to this approach are illustrated by the recent report from Ogawa et al. in which a dual-modal agent for imaging, using trastuzumab and panitumumab for targeting, was described.⁵³ Tumor targeting was demonstrated by optical imaging and planar γ -scintigraphy, although the quality of the radiolabeled products is questionable. The data presented %ID/g uptake of ^{111}In -trastuzumab in the spleen and liver that was higher than what was obtained in the tumor. This is also evident in the γ -scintigraphic images and indicates that either the mAb was compromised by the modification or the bifunctional chelate was inadequate or both. In addition, characterization such as the number of chelate or dye molecules per mAb molecule was not presented. This aspect is often overlooked, yet it is well-documented that modification of a mAb can potentially alter its immunoreactivity and metabolic processing, and thus targeting and uptake into target tissue.⁵⁶

An alternate strategy involves synthesis of a trifunctional molecule that contains a group that will react with a targeting agent,

an optical dye and a chelate that will complex with a radionuclide. This latter approach should simplify the characterization of the modified agent since there is a 1:1 relationship between the dye and the radionuclide.

As mentioned earlier, patients are selected for trastuzumab therapy based on the HER2 scoring of tumor biopsies by immunohistochemical techniques; only those with scores of 3+ or 2+ are considered for trastuzumab therapy. In spite of this pre-selection criteria, the percentage of patients that respond to trastuzumab as a single agent is quite low (12–35%). When combined with anthracyclines or taxanes, the percentage of responders increases to as high as 60%.³ Using breast cancer xenograft mouse models, McLarty et al. were able to distinguish HER2 expression levels with ^{111}In -trastuzumab.²⁴ The investigators were also able to associate responsiveness to trastuzumab with uptake of the radiolabeled trastuzumab. The differentiation, however, required corrections for tumor uptake and radioactivity in the blood using a non-specific antibody, a scenario that might not be easily accomplished in patients. Studies are ongoing within this laboratory evaluating and comparing the level of HER2 expression in the various tumor xenografts with the level of ^{111}In -trastuzumab uptake.

The six tumor models presented in this report ranged in the degree of RIC targeting, as well as in the timing of peak targeting. Successful therapy or imaging, using radiolabeled trastuzumab requires neither a high expression of HER2 by a patient's tumor nor expression of HER2 by every cell. In the arena of therapy, radioactive decay is omni-directional and neighboring cells, whether expressing the HER2 target or not, may receive a therapeutic dose of radiation (the “bystander effect”).⁵⁷ In the case of imaging, again, not all cells in a tumor mass need to either express HER2 or express HER2 at high levels for adequate signal to be produced for detection of tumor masses. This is the basic premise of advancing ^{111}In -trastuzumab into an imaging study at the NCI and a therapy study with ^{212}Pb -trastuzumab at the University of Alabama. The data presented here is not only the foundation for these two clinical studies, but also demonstrates the potential of radiolabeled trastuzumab in the treatment and management of cancer patients. Thus, the utility of radiolabeled trastuzumab should not be limited solely to the diagnosis and treatment of breast cancer patients, nor should it be restricted to just those patients with higher levels of HER2 expression.

Materials and Methods

Cell lines. In vivo studies were conducted using human carcinoma cell lines of the colon (LS-174T and HT-29; provided by Dr. J. Greiner, NCI), pancreas (PC-Sw; obtained from Dr. JB Mitchell, NCI), prostate (DU-145 and PC-3), ovary (SKOV-3) and a melanoma cell line (A375). All cell lines, unless stated otherwise, were obtained from ATCC (Manassas, VA). LS-174T was grown in Dulbecco's minimum essential medium (DMEM) supplemented with 10 mM glutamine.⁵⁸ SKOV-3 were maintained in McCoy's 5a medium and A375 cells in DMEM with 1 mM sodium pyruvate.⁵⁹ PC-Sw, PC-3 and DU-145 were grown in RPMI-1640.^{45,60} All media were also supplemented with 10%

FetalPlex (Gemini Bio-Products, Woodland, CA, USA) and 1 mM non-essential amino acids. Media and supplements were obtained from Quality Biologicals (Gaithersburg, MD, USA), Invitrogen (Carlsbad, CA, USA) or Lonza (Walkersville, MD, USA).

Chelate synthesis and mAb conjugation. The synthesis, characterization and purification of the bifunctional ligand, CHX-A⁹-DTPA, used as the radiometal chelate, has been previously described.⁶¹ Conjugation of trastuzumab with CHX-A⁹-DTPA was accomplished by methods previously published using a 10:1 molar ratio of chelate to trastuzumab in the reaction.^{61,62} HuIgG (MP Biomedicals, Santa Ana, CA, USA) was also conjugated with CHX-A⁹-DTPA at a 10:1 molar ratio, resulting in a final chelate-to-protein ratio of 1.7. The HuIG-CHX-A⁹ served as a non-specific antibody in the tumor targeting studies. The final concentration of trastuzumab was quantified by the method of Lowry using a BSA standard.⁶³ The average number of CHX-A⁹-DTPA molecules linked to the mAb was determined using a spectrophotometric assay based on the titration of yttrium-Arsenazo(III) complex.⁶⁴

Radiolabeling. Radiolabeling of CHX-A⁹-trastuzumab (50 µg in 100 µL of 0.15 M NH₄OAc buffer, pH 7.0) with ¹¹¹In was performed by adding 0.5–1 mCi in 1–2 µL of ¹¹¹In Cl (in 0.05 M HCl) (PerkinElmer, Shelton, CT, USA).^{45,62} The reaction was quenched after 30 min with 0.1 M EDTA (3 µL) to scavenge free radiometal and the radiolabeled product was purified using a PD-10 desalting column (GE Healthcare, Piscataway, NJ, USA).

⁸⁶Yttrium, produced as previously described, was generously provided by the Washington University School of Medicine.⁶⁵ CHX-A⁹-DTPA-Trastuzumab (50 µg in 0.15 M NH₄OAc) was added to the ⁸⁶Y solution (3.8–4.6 mCi in 0.1 M nitric acid, 500 µL) containing ascorbic acid (50 µL, 220 µg/µL) that had been neutralized to pH 5–6 with NH₄OAc buffer (50 µL 5 M, pH 7.0). After a 30 min incubation at ambient temperature, the mixture, vortexed briefly and incubated at room temperature for 30 min. The reaction was quenched and the radiolabeled product was purified using a PD-10 desalting column.

Radio-iodination of trastuzumab with ¹²⁵I was performed using Iodo-Gen (Pierce Chemical, Rockford, IL, USA).⁶⁶ Briefly, a solution of Na¹²⁵I (0.5–1 mCi) was added to a solution of trastuzumab (50 µg) in phosphate buffer (100 µL, 0.1 M, pH 7) contained in a test tube pre-coated with Iodo-Gen. The radio-iodinated product was purified as above using a PD-10 desalting column after 3 min incubation at room temperature. Integrity of the final radiolabeled products was evaluated by size-exclusion chromatography using an analytical TSK-3000SW column (Tosoh Bioscience, Montgomeryville, PA, USA) eluted at a flow rate of 0.5 mL/min.

Radioimmunoassays. The immunoreactivity of the trastuzumab-CHX-A⁹-DTPA conjugate was evaluated in a competition radioimmunoassay as described elsewhere.⁶⁷ 96-well plates were seeded with SKOV-3 cells (~3 x 10³ in 100 µL) and incubated for 4–5 days until ~80% confluency was attained. The cells were fixed with 80% cold methanol (200 µL), after 1 h at 4°C, the wells were washed with PBS and PBS/BSA (150 µL) added to each well and allowed to sit for an additional hour at

ambient temperature. The wells were aspirated and serial dilutions (0.08–5,000 ng in 50 µL BSA/PBS) of unmodified trastuzumab or trastuzumab-CHX-A⁹-DTPA conjugate were added to the wells in triplicate, one set of wells received BSA/PBS without any competitor, along with ¹²⁵I-trastuzumab (~100,000 cpm in 50 µL BSA/PBS). Following an overnight incubation at ambient temperature, the wells were washed three times with BSA/PBS. The bound radioactivity was removed with 100 µL 0.2 M NaOH, transferred to 12 x 75 mm tubes and counted in a γ-scintillation counter (Wizard One, PerkinElmer, Shelton, CT, USA). The percent inhibition was calculated using the buffer control and plotted. HuM195, an anti-CD33 mAb provided by Dr. M. McDevitt, Memorial Sloan-Kettering Cancer Center, served as a negative control.

The immunoreactivity of the ¹¹¹In-trastuzumab was assessed in a radioimmunoassay as detailed previously using methanol-fixed SKOV-3 cells.⁴⁵ Serial dilutions of ¹¹¹In-trastuzumab (~300,000 to ~12,500 cpm in 50 µL of BSA/PBS) were added to 12 x 75 mm test tubes containing SKOV-3 cells (1 x 10⁶/50 µL PBS/BSA) and left for 18 h at ambient temperature. The cells were then washed, pelleted and counted in a γ-scintillation counter. The percentage binding was calculated for each dilution and averaged. The specificity of the radiolabeled trastuzumab was confirmed by incubating one set of cells with radiolabeled trastuzumab and 10 µg of unlabeled trastuzumab.

In vivo studies. All in vivo studies were performed using 4–6 week old female or male athymic (nu/nu) mice (Charles River Laboratories, Wilmington, DE, USA). All animal protocols were approved by the NCI Animal Care and Use Committee.

Tumor targeting. Mice were injected s.c. in the right rear leg with either 2 x 10⁶ LS-174T cells or 4 x 10⁶ PC-Sw, SKOV-3, DU-145, HT-29, PC-3 or A375 cells in media (200 µL) with 20% Matrigel (BD Biosciences, San Jose, CA, USA). Mice were utilized in studies when the tumor xenografts maximal diameter measured 0.4–0.6 cm. Mice (n = 5 per time point) were injected i.v. with ¹¹¹In-CHX-A⁹-trastuzumab (~7.5 µCi/2.3 µg trastuzumab) and sacrificed by exsanguination at time points from 24–168 h. The i.p. model entailed injecting mice with 1 x 10⁸ cells in 1 mL of media. The mice bearing the i.p. xenografts were then utilized in studies 5 d post-tumor implantation. In all studies, the blood, tumor and major organs were collected, wet-weighted and counted in a γ-scintillation counter. The percent injected dose per gram (%ID/g) and standard deviation were calculated.

Pharmacokinetics. Blood pharmacokinetics were performed with both non-tumor-bearing (n = 5) and mice bearing s.c. LS-174T tumors (n = 5). Following i.v. (0.2 mL) or i.p. (0.5 mL) injection of ~7.5 µCi ¹¹¹In-CHX-A⁹-trastuzumab, blood samples were collected at various time points via the tail vein in heparinized capillary tubes (10 µL; Drummond Scientific, Broomall, PA). The blood was transferred to a cotton filter, placed in a 12 x 75 mm tube and the radioactivity measured in a γ-scintillation counter. The percent injected dose per mL of blood was calculated for each of the samples; the averages and standard deviations were calculated and plotted. The T_{1/2}α and T_{1/2}β were calculated using Sigmaplot 2001 Version 7.101 (SPSS, Inc., San Jose, CA).

γ -Scintigraphy. Radioimmunosciintigraphy was performed with mice bearing s.c. LS-174T PC-Sw, HT-29, DU-145, SKOV-3, PC-3 and A375 xenografts to further validate tumor targeting with $^{111}\text{In-CHX-A}^{\text{trastuzumab}}$. Tumor-bearing mice ($n = 4-5$) were given i.v. injections of $^{111}\text{In-CHX-A}^{\text{trastuzumab}}$ ($-80-100 \mu\text{Ci}$ on $6-7.5 \mu\text{g}$) in $200 \mu\text{L}$ of PBS. The mice were chemically restrained with 1.5% isoflurane (Abbott Laboratories, NJ) delivered in O_2 using a Summit Anesthesia Solutions vaporizer (Bend, OR) at a flow rate of $\sim 1.0 \text{ L/min}$. Images (100,000 counts) were acquired 24–168 h post-injection with a large field of view (LFOV) gamma camera equipped with a pinhole collimator using a 20% window centered on both photopeaks (173 and 247 KeV).⁶⁸

Positron-emission tomography. Small animal positron-emission tomography (PET) studies were performed using the ATLAS (Advanced Technology Laboratory Animal Scanner) at the National Institutes of Health, Bethesda, MD USA. Whole body imaging studies (6 bed positions, total acquisition time of 1 h per mouse) were carried out on mice anesthetized with 1.5% isoflurane on a temperature-controlled bed as previously described.⁶⁹ Briefly, LS-174T tumor-bearing female athymic

mice were injected i.v. and i.p (for s.c. and i.p tumors xenografts, respectively) with $\sim 100 \mu\text{Ci}$ of $^{86}\text{Y-CHX-A}^{\text{trastuzumab}}$. For mice bearing i.p tumors, the active dataset was filtered using the 3-D median filter method (kernel size = 3) to preserve the edges while removing background noise. The reconstructed images were processed and analyzed using AMIDE (A Medical Image Data Examiner) software program. To minimize spillover effects, regions of interest (ROIs) were drawn to enclose approximately 80–90% of the organ of interest, avoiding the edges. To minimize partial-volume effects caused by non-uniform distribution of the radioactivity in the containing volume, smaller ROIs were consistently drawn to enclose the organ. After imaging, the mice were euthanized and biodistribution studies were performed to determine the correlation between PET-assessed in vivo %ID/cc and biodistribution determined %ID/g.

Acknowledgements

This research was supported by the Intramural Research Program of the NIH, National Cancer Institute, Center for Cancer Research. The production of ^{86}Y at Washington University School of Medicine is supported by the NCI grant R24 CA86307.

References

- Wolff AC, Hammond ME, Schwartz JN, Hagerty KL, Allred DC, Cote RJ, et al. American Society of Clinical Oncology/College of American Pathologists guideline recommendations for human epidermal growth factor receptor 2 testing in breast cancer. *J Clin Oncol* 2007; 25:118-45.
- Press MF, Pike MC, Chazin VR, Hung G, Udove JA, Markowicz M, et al. Her-2/neu expression in node-negative breast cancer: direct tissue quantitation by computerized image analysis and association of overexpression with increased risk of recurrent disease. *Cancer Res* 1993; 53:4960-70.
- Shepard HM, Jin P, Slamon D, Pirot Z, Maneval DC. Herceptin. In: Y. Chernajovsky, Nissim A, Ed(s). *Therapeutic Antibodies. Handbook of Experimental Pharmacology*. Berlin Heidelberg: Springer-Verlag 2008; 183-219.
- Ellis LM, Hicklin DJ. Resistance to Targeted Therapies: Refining Anticancer Therapy in the Era of Molecular Oncology. *Clin Cancer Res* 2009; 15:7471-8.
- Pohlmann PR, Mayer IA, Mernaugh R. Resistance to Trastuzumab in Breast Cancer. *Clin Cancer Res* 2009; 15:7479-91.
- Azzam EI, de Toledo SM, Little JB. Stress signaling from irradiated to non-irradiated cells. *Curr Cancer Drug Targets* 2004; 4:53-64.
- Prise KM, Folkard M, Michael BD. Bystander responses induced by low LET radiation. *Oncogene* 2003; 22:7043-9.
- Jain RK. Vascular and interstitial barriers to delivery of therapeutic agents in tumors. *Cancer Metastasis Rev* 1990; 9:253-66.
- Yokota T, Milenic DE, Whitlow M, Schlom J. Rapid tumor penetration of a single-chain Fv and comparison with other immunoglobulin forms. *Cancer Res* 1992; 52:3402-8.
- Ballangrud AM, Yang WH, Palm S, Enmon R, Borchardt PE, Pellegrini VA, et al. Alpha-particle emitting atomic generator (Actinium-225)-labeled trastuzumab (herceptin) targeting of breast cancer spheroids: efficacy versus HER2/neu expression. *Clin Cancer Res* 2004; 10:4489-97.
- Crow DM, Williams L, Colcher D, Wong JY, Raubitschek A, Shively JE. Combined radioimmunotherapy and chemotherapy of breast tumors with Y-90-labeled anti-Her2 and anti-CEA antibodies with taxol. *Bioconjug Chem* 2005; 16:1117-25.
- Lub-de Hooge MN, Kosterink JG, Perik PJ, Nijhuis H, Tran L, Bart J, et al. Preclinical characterisation of $^{111}\text{In-DTPA-trastuzumab}$. *Br J Pharmacol* 2004; 143:99-106.
- Milenic DE, Garmestani K, Brady ED, Albert PS, Ma D, Abdulla A, et al. Targeting of HER2 Antigen for the Treatment of Disseminated Peritoneal Disease. *Clin Cancer Res* 2004; 23:7834-41.
- Milenic DE, Garmestani K, Brady ED, Albert PS, Abdulla A, Flynn J, et al. Potentiation of high-LET radiation by gemcitabine: targeting HER2 with trastuzumab to treat disseminated peritoneal disease. *Clin Cancer Res* 2007; 13:1926-35.
- Milenic DE, Garmestani K, Brady ED, Albert PS, Ma D, Abdulla A, et al. Alpha-particle radioimmunotherapy of disseminated peritoneal disease using a (212)Pb-labeled radioimmunoconjugate targeting HER2. *Cancer Biother Radiopharm* 2005; 20:557-68.
- Palm S, Back T, Claesson I, Danielsson A, Elgqvist J, Frost S, et al. Therapeutic efficacy of astatine-211-labeled trastuzumab on radioresistant SKOV-3 tumors in nude mice. *Int J Radiat Oncol Biol Phys* 2007; 69:572-9.
- Palm S, Enmon RM Jr, Matei C, Kolbert KS, Xu S, Zanzonico PB, et al. Pharmacokinetics and Biodistribution of (86)Y-Trastuzumab for (90)Y dosimetry in an ovarian carcinoma model: correlative MicroPET and MRI. *J Nucl Med* 2003; 44:1148-55.
- Tang Y, Wang J, Scollard DA, Mondal H, Holloway C, Kahn HJ, et al. Imaging of HER2/neu-positive BT-474 human breast cancer xenografts in athymic mice using (111)In-trastuzumab (Herceptin) Fab fragments. *Nucl Med Biol* 2005; 32:51-8.
- Tsai SW, Sun Y, Williams LE, Raubitschek AA, Wu AM, Shively JE. Biodistribution and radioimmunotherapy of human breast cancer xenografts with radiometal-labeled DOTA conjugated anti-HER2/neu antibody 4D5. *Bioconjug Chem* 2000; 11:327-34.
- de Korte MA, de Vries EG, Lub-de Hooge MN, Jager PL, Gietema JA, van der Graaf WT, et al. $^{111}\text{Indium-trastuzumab}$ visualises myocardial human epidermal growth factor receptor 2 expression shortly after anthracycline treatment but not during heart failure: a clue to uncover the mechanisms of trastuzumab-related cardiotoxicity. *Eur J Cancer* 2007; 43:2046-51.
- Dijkers EC, Kosterink JG, Rademaker AP, Perk LR, van Dongen GA, Bart J, et al. Development and characterization of clinical-grade $^{89}\text{Zr-trastuzumab}$ for HER2/neu immunoPET imaging. *J Nucl Med* 2009; 50:974-81.
- Garmestani K, Milenic DE, Plascjak PS, Brechbiel MW. A new and convenient method for purification of ^{86}Y using a Sr(II) selective resin and comparison of biodistribution of ^{86}Y and ^{111}In labeled Herceptin. *Nucl Med Biol* 2002; 29:599-606.
- Gee MS, Upadhyay R, Bergquist H, Alencar H, Reynolds F, Maricovich M, et al. Human breast cancer tumor models: molecular imaging of drug susceptibility and dosing during HER2/neu-targeted therapy. *Radiology* 2008; 248:925-35.
- McLarty K, Cornelissen B, Scollard DA, Done SJ, Chun K, Reilly RM. Associations between the uptake of $^{111}\text{In-DTPA-trastuzumab}$, HER2 density and response to trastuzumab (Herceptin) in athymic mice bearing subcutaneous human tumour xenografts. *Eur J Nucl Med Mol Imaging* 2009; 36:81-93.
- Niu G, Li Z, Cao Q, Chen X. Monitoring therapeutic response of human ovarian cancer to 17-DMAG by noninvasive PET imaging with (64)Cu-DOTA-trastuzumab. *Eur J Nucl Med Mol Imaging* 2009; 36:1510-9.
- Perik PJ, Lub-De Hooge MN, Gietema JA, van der Graaf WT, de Korte MA, Jonkman S, et al. Indium-111-labeled trastuzumab scintigraphy in patients with human epidermal growth factor receptor 2-positive metastatic breast cancer. *J Clin Oncol* 2006; 24:2276-82.
- Robinson MK, Doss M, Shaller C, Narayanan D, Marks JD, Adler LP, et al. Quantitative immunopositron emission tomography imaging of HER2-positive tumor xenografts with an iodine-124 labeled anti-HER2 diabody. *Cancer Res* 2005; 65:1471-8.

28. Smith-Jones PM, Solit D, Afroze F, Rosen N, Larson SM. Early tumor response to Hsp90 therapy using HER2 PET: comparison with 18F-FDG PET. *J Nucl Med* 2006; 47:793-6.
29. Smith-Jones PM, Solit DB, Akhurst T, Afroze F, Rosen N, Larson SM. Imaging the pharmacodynamics of HER2 degradation in response to Hsp90 inhibitors. *Nat Biotechnol* 2004; 22:701-6.
30. Agus DB, Bunn PA Jr, Franklin W, Garcia M, Ozols RF. HER-2/neu as a therapeutic target in non-small cell lung cancer, prostate cancer and ovarian cancer. *Semin Oncol* 2000; 27:53-63.
31. Natali PG, Nicotra MR, Bigotti A, Venturo I, Slamon DJ, Fendly BM, et al. Expression of the p185 encoded by HER2 oncogene in normal and transformed human tissues. *Int J Cancer* 1990; 45:457-61.
32. Press MF, Cordon-Cardo C, Slamon DJ. Expression of the HER-2/neu proto-oncogene in normal human adult and fetal tissues. *Oncogene* 1990; 5:953-62.
33. Ross JS, McKenna BJ. The HER-2/neu oncogene in tumors of the gastrointestinal tract. *Cancer Invest* 2001; 19:554-68.
34. Slamon D, Pegram M. Rationale for trastuzumab (Herceptin) in adjuvant breast cancer trials. *Semin Oncol* 2001; 28:13-9.
35. De Santes K, Slamon D, Anderson SK, Shepard M, Fendly B, Maneval D, et al. Radiolabeled antibody targeting of the HER-2/neu oncoprotein. *Cancer Res* 1992; 52:1916-23.
36. Elgqvist J, Andersson H, Haglund E, Jensen H, Kahu H, Lindegren S, et al. Intraperitoneal alpha-radioimmunotherapy in mice using different specific activities. *Cancer Biother Radiopharm* 2009; 24:509-13.
37. Kotts CE, Su FM, Leddy C, Dodd T, Scates S, Shalaby MR, et al. ¹⁸⁶Re-labeled antibodies to p185HER2 as HER2-targeted radioimmunopharmaceutical agents: comparison of physical and biological characteristics with ¹²⁵I and ¹³¹I-labeled counterparts. *Cancer Biother Radio* 1996; 11:133-44.
38. Herbertson RA, Tebbutt NC, Lee FT, MacFarlane DJ, Chappell B, Micallef N, et al. Phase I biodistribution and pharmacokinetic study of Lewis Y-targeting immunoconjugate CMD-193 in patients with advanced epithelial cancers. *Clin Cancer Res* 2009; 15:6709-15.
39. Kossman SE, Scheinberg DA, Jurcic JG, Jimenez J, Caron PC. A phase I trial of humanized monoclonal antibody HuM195 (anti-CD33) with low-dose interleukin 2 in acute myelogenous leukemia. *Clin Cancer Res* 1999; 5:2748-55.
40. Scott AM, Lee FT, Tebbutt N, Herbertson R, Gill SS, Liu Z, et al. A phase I clinical trial with monoclonal antibody ch806 targeting transitional state and mutant epidermal growth factor receptors. *P Natl Acad Sci USA* 2007; 104:4071-6.
41. Scott AM, Tebbutt N, Lee FT, Cavicchiolo T, Liu Z, Gill S, et al. A phase I biodistribution and pharmacokinetic trial of humanized monoclonal antibody Hu3s193 in patients with advanced epithelial cancers that express the Lewis-Y antigen. *Clin Cancer Res* 2007; 13:3286-92.
42. Camera L, Kinuya S, Garmestani K, Wu C, Brechbiel MW, Pai LH, et al. Evaluation of the serum stability and in vivo biodistribution of CHX-DTPA and other ligands for yttrium labeling of monoclonal antibodies. *J Nucl Med* 1994; 35:882-9.
43. Milenic DE, Garmestani K, Chappell LL, Dadachova E, Yordanov A, Ma D, et al. In vivo comparison of macrocyclic and acyclic ligands for radiolabeling of monoclonal antibodies with ¹⁷⁷Lu for radioimmunotherapeutic applications. *Nucl Med Biol* 2002; 29: 431-42.
44. Milenic DE, Roselli M, Mirzadeh S, Pippin CG, Gansow OA, Colcher D, et al. In vivo evaluation of bismuth-labeled monoclonal antibody comparing DTPA-derived bifunctional chelates. *Cancer Biother Radio* 2001; 16:133-46.
45. Milenic DE, Wong KJ, Baidoo KE, Ray GL, Garmestani K, Williams M, et al. Cetuximab: preclinical evaluation of a monoclonal antibody targeting EGFR for radioimmunodiagnostic and radioimmunotherapeutic applications. *Cancer Biother Radio* 2008; 23:619-31.
46. Ray GL, Baidoo KE, Wong KJ, Williams M, Garmestani K, Brechbiel MW, et al. Preclinical evaluation of a monoclonal antibody targeting the epidermal growth factor receptor as a radioimmunodiagnostic and radioimmunotherapeutic agent. *Br J Pharmacol* 2009; 157:1541-8.
47. Rowlinson G, Snook D, Busza A, Epenetos AA. Antibody-guided localization of intraperitoneal tumors following intraperitoneal or intravenous antibody administration. *Cancer Res* 1987; 47:6528-31.
48. Wahl RL, Barrett J, Geatzi O, Liebert M, Wilson BS, Fisher S, et al. The intraperitoneal delivery of radiolabeled monoclonal antibodies: studies on the regional delivery advantage. *Cancer Immunol Immunother* 1988; 26:187-201.
49. Sgouros G, Ballangrud AM, Jurcic JG, McDevitt MR, Humm JL, Erdi YE, et al. Pharmacokinetics and dosimetry of an alpha-particle emitter labeled antibody: ²¹³Bi-HuM195 (anti-CD33) in patients with leukemia. *J Nucl Med* 1999; 40:1935-46.
50. Dijkers EC, Oude Munnink TH, Kosterink JG, Brouwers AH, Jager PL, de Jong JR, et al. Biodistribution of ⁸⁹Zr-trastuzumab and PET imaging of HER2-positive lesions in patients with metastatic breast cancer. *Clin Pharmacol Ther* 87:586-92.
51. Kramer-Marek G, Kiesewetter DO, Martiniova L, Jagoda E, Lee SB, Capala J. [¹⁸F]FBEM-Z(HER2:342)-Affibody molecule-a new molecular tracer for in vivo monitoring of HER2 expression by positron emission tomography. *Eur J Nucl Med Mol Imaging* 2008; 35:1008-18.
52. Orlova A, Wallberg H, Stone-Elander S, Tolmachev V. On the selection of a tracer for PET imaging of HER2-expressing tumors: direct comparison of a ¹²⁴I-labeled affibody molecule and trastuzumab in a murine xenograft model. *J Nucl Med* 2009; 50:417-25.
53. Ogawa M, Regino CA, Seidel J, Green MV, Xi W, Williams M, et al. Dual-modality molecular imaging using antibodies labeled with activatable fluorescence and a radionuclide for specific and quantitative targeted cancer detection. *Bioconjug Chem* 2009; 20:2177-84.
54. Sampath L, Kwon S, Ke S, Wang W, Schiff R, Mawad ME, et al. Dual-labeled trastuzumab-based imaging agent for the detection of human epidermal growth factor receptor 2 overexpression in breast cancer. *J Nucl Med* 2007; 48:1501-10.
55. Xu H, Eck PK, Baidoo KE, Choyke PL, Brechbiel MW. Toward preparation of antibody-based imaging probe libraries for dual-modality positron emission tomography and fluorescence imaging. *Bioorg Med Chem* 2009; 17:5176-81.
56. Esteban JM, Schlom J, Gansow OA, Atcher RW, Brechbiel MW, Simpson DE, et al. New method for the chelation of indium-111 to monoclonal antibodies: biodistribution and imaging of athymic mice bearing human colon carcinoma xenografts. *J Nucl Med* 1987; 28:861-70.
57. Lorimore SA, Coates PJ, Wright EG. Radiation-induced genomic instability and bystander effects: inter-related nontargeted effects of exposure to ionizing radiation. *Oncogene* 2003; 22:7058-69.
58. Tom BH, Rutzky LH, Jakstys MH. Human colonic adenocarcinoma cells. Establishment and description of a new cell line. *In Vitro* 1976; 12:180-91.
59. Mandler R, Kobayashi H, Hinson ER, Brechbiel MW, Waldmann TA. Herceptin-geldanamycin immunoconjugates: pharmacokinetics, biodistribution and enhanced antitumor activity. *Cancer Res* 2004; 64:1460-7.
60. Cook JA, Choudhuri R, Degraff W, Gamson J, Mitchell JB. Halofuginone enhances the radiation sensitivity of human tumor cell lines. *Cancer Lett* 289:119-26.
61. Wu C, Kobayashi H, Sun B, Yoo TM, Paik CH, Gansow OA, et al. Stereochemical influence on the stability of radio-metal complexes in vivo. Synthesis and evaluation of the four stereoisomers of 2-(p-nitrobenzyl)-trans-CyDTPA. *Bioorg Med Chem* 1997; 5:1925-34.
62. Garmestani K, Yao Z, Zhang M, Wong K, Park CW, Pastan I, et al. Synthesis and evaluation of a macrocyclic bifunctional chelating agent for use with bismuth radionuclides. *Nucl Med Biol* 2001; 28:409-18.
63. Lowry OH, Rosebrough NJ, Farr AL, Randall RJ. Protein measurement with the folin phenol reagent 1951; 193:265-75.
64. Pippin CG, Parker TA, McMurry TJ, Brechbiel MW. Spectrophotometric method for the determination of a bifunctional DTPA ligand in DTPA-monoclonal antibody conjugates. *Bioconjug Chem* 1992; 3:342-5.
65. Yoo J, Tang L, Perkins TA, Rowland DJ, Laforest R, Lewis JS, et al. Preparation of high specific activity (86)Y using a small biomedical cyclotron. *Nucl Med Biol* 2005; 32:891-7.
66. Fraker PJ, Speck JC Jr. Protein and cell membrane iodinations with a sparingly soluble chloroamide, 1,3,4,6-tetrachloro-3a,6a-diphrenylglycoluril. *Biochem Biophys Res Commun* 1978; 80:849-57.
67. Xu H, Baidoo K, Gunn AJ, Boswell CA, Milenic DE, Choyke PL, et al. Design, synthesis and characterization of a dual modality positron emission tomography and fluorescence imaging agent for monoclonal antibody tumor-targeted imaging. *J Med Chem* 2007; 50:4759-65.
68. Camera L, Kinuya S, Garmestani K, Pai LH, Brechbiel MW, Gansow OA, et al. Evaluation of a new DTPA-derivative chelator: comparative biodistribution and imaging studies of ¹¹¹In-labeled B3 monoclonal antibody in athymic mice bearing human epidermoid carcinoma xenografts. *Nucl Med Biol* 1993; 20:955-62.
69. Nayak TK, Regino CA, Wong KJ, Milenic DE, Garmestani K, Baidoo KE, et al. PET imaging of HER1-expressing xenografts in mice with (86)Y-CHX-A'-DTPA-cetuximab. *Eur J Nucl Med Mol Imaging* 2010; 37:1368-76.